Lawrence Berkeley National Laboratory

Recent Work

Title

INVESTIGATION OF HIGH SPIN LEVELS PREFERENTIALLY POPULATED BY THE (a,a) REACTION

Permalink

https://escholarship.org/uc/item/3z7312z3

Authors

Rivet, Ernest
Pehl, Richard H.
Cerny, Joseph
et al.

Publication Date

1965-06-01

eScholarship.org Powered by the California Digital Library
University of California

UCRL-16200

University of California

Ernest O. Lawrence Radiation Laboratory

INVESTIGATION OF HIGH SPIN LEVELS PREFERENTIALLY POPULATED BY THE (α, d) REACTION

TWO-WEEK LOAN COPY

This is a Library Circulating Copy which may be borrowed for two weeks. For a personal retention copy, call Tech. Info. Division, Ext. 5545

Berkeley, California

DISCLAIMER

This document was prepared as an account of work sponsored by the United States Government. While this document is believed to contain correct information, neither the United States Government nor any agency thereof, nor the Regents of the University of California, nor any of their employees, makes any warranty, express or implied, or assumes any legal responsibility for the accuracy, completeness, or usefulness of any information, apparatus, product, or process disclosed, or represents that its use would not infringe privately owned rights. Reference herein to any specific commercial product, process, or service by its trade name, trademark, manufacturer, or otherwise, does not necessarily constitute or imply its endorsement, recommendation, or favoring by the United States Government or any agency thereof, or the Regents of the University of California. The views and opinions of authors expressed herein do not necessarily state or reflect those of the United States Government or any agency thereof or the Regents of the University of California.

Submitted to Physical Review

UCRL-16200

UNIVERSITY OF CALIFORNIA

Lawrence Radiation Laboratory
Berkeley, California

AEC Contract No. W-7405-eng-48

INVESTIGATION OF HIGH SPIN LEVELS PREFERENTIALLY POPULATED BY THE (α,d) REACTION

Ernest Rivet, Richard H. Pehl,
Joseph Cerny, and Bernard G. Harvey

June 1965

INVESTIGATION OF HIGH SPIN LEVELS PREFERENTIALLY POPULATED BY THE (α,d) REACTION*

Ernest Rivet,† Richard H. Pehl,
Joseph Cerny, and Bernard G. Harvey

Lawrence Radiation Laboratory and
Department of Chemistry
University of California
Berkeley, California

June 1965

ABSTRACT

The energy spectra of deuterons from the (α,d) reaction on C^{12}, N^{14}, N^{15}, O^{16}, Ne^{20}, Mg^{24}, Mg^{26}, Si^{28}, S^{32}, Ar^{40}, and Ca^{40} have been observed. These reactions were induced by alpha particles ranging in energy from 42 to 53 MeV. All the energy spectra were dominated by one or more preferentially populated levels. Evidence that these levels have a common configuration is obtained from (a) the relationship between their Q values of formation and the mass number of the recoil nuclei, and (b) the similarity of their angular distributions. It is proposed that the levels preferentially populated are of a $[J_T + (j_p j_n)_{J'}]_J$ configuration, with the proton-neutron pair captured in the $d_{5/2}$ or $f_{7/2}$ shell, and that the maximum final spin (5, 6, or 7) is favored.

A self-consistent energy-level scheme for the low-lying levels of Sc^{42} is also proposed.

I. INTRODUCTION

In terms of a direct stripping mechanism, the (α,d) reaction will populate levels that correspond to a proton-neutron pair coupled to an undisturbed target core. Further selectivity will arise from the degree of similarity existing between the wave function of the proton-neutron pair in the captured state and the wave function of the proton-neutron pair in the alpha particle.

In a previous investigation of the (α,d) reaction on the target nuclei C^{12}, N^{14}, N^{15}, and O^{16} the presence of preferentially populated levels was reported.[1] It was concluded that these levels arose from the proton-neutron pair being captured as a "deuteron" in the $d_{5/2}$ shell corresponding to a $[J_T + (d_{5/2})^2_5]_J$ configuration, where J_T—the angular momentum of the target nucleus—is coupled with the spin brought in by the captured particles, giving J—the spin of the final state(s).

The $C^{12}(\alpha,d)N^{14}$, $N^{14}(\alpha,d)O^{16}$, and $O^{16}(\alpha,d)F^{18}$ reactions have now been observed under better experimental conditions, and levels of $(d_{5/2})^2_5$ character have also been observed in the $Ne^{20}(\alpha,d)Na^{22}$ and $Mg^{24}(\alpha,d)Al^{26}$ reactions. This investigation was also continued to the $f_{7/2}$ shell to extend the usefulness of the earlier ideas.[1] Preferentially populated levels which probably correspond to $[J_T + (d_{5/2}\ f_{7/2})_6]_J$ and/or $[J_T + (f_{7/2})^2_7]_J$ configurations were observed in the $Ne^{20}(\alpha,d)Na^{22}$, $Mg^{24}(\alpha,d)Al^{26}$, $Mg^{26}(\alpha,d)Al^{28}$, $Si^{28}(\alpha,d)P^{30}$, $S^{32}(\alpha,d)Cl^{34}$, $Ca^{40}(\alpha,d)Sc^{42}$ and $Ar^{40}(\alpha,d)K^{42}$ reactions.

II. EXPERIMENTAL

The 42 to 53 MeV beams of alpha particles used to induce the various (α,d) reactions were provided by the Berkeley 88-inch spiral ridge cyclotron. The general beam transport system has been described previously.[2]

For all these reactions the particles were detected by a counter-telescope that consisted of two lithium-drifted silicon crystals. In the case of the $Ne^{20}(\alpha,d)Na^{22}$, $Ca^{40}(\alpha,d)Sc^{42}$, and $Ar^{40}(\alpha,d)K^{42}$ reactions the signals from a 1.25 mm transmission counter and a 2.25 mm stopping counter were added and sent to a 400 channel RIDL pulse-height analyzer. The particle identification was performed electronically by an analog pulse multiplier. For the (α,d) reactions studied on the C^{12}, N^{14}, O^{16}, Mg^{24}, Mg^{26}, and Si^{28} target nuclei the counter telescope consisted of a 0.35 mm transmission counter placed in front of a 3.0 mm stopping counter. To increase the effective counter thickness, the counter telescope was rotated 40 deg with respect to the flight path of the scattered particles. Identification of the reaction products was performed by a particle identifier[3] that employs the empirical relationship,

$$\text{Range} = a\, E^{1.73}$$

where a depends on the nature of the particle and E is its incident energy. A typical identifier spectrum is shown in Fig. 1. Total-energy pulses were fed into a 4096-channel Nuclear Data pulse-height analyzer which was routed so that the deuteron and triton spectra were recorded simultaneously, each in a 1024-channel group. Pulses that corresponded to

the proton-deuteron valley were routed into a third 1024-channel group to record any possible loss of deuterons. The overall block diagram has been published.[4] Energy resolutions of about 200 keV were obtained for solid targets.

The beam intensity, which ranged from 15 to 280 mμA depending upon the angle of observation, was measured by means of a Faraday cup and integrating electrometer. A lithium-drifted silicon detector placed at a fixed angle (≈20 deg) was used to observe the elastically scattered alphas, and thus monitored the target thickness and determined the "quality" of the beam.

Different methods were used in preparing the various targets. The C^{12} targets were prepared from a solution of colloidal graphite in alcohol and acetone.[4] Self-supporting films about 0.3 mg/cm^2 thick were obtained with this method. Most of the oxygen impurity was removed by heating the films to 1400°C in vacuum and cooling to 200°C before exposure to the atmosphere. Self-supporting Mg^{24}, Mg^{26}, and Si^{28} targets 1.38, 1.1, and 0.043 mg/cm^2 thick, respectively, were prepared by evaporation. Separated isotopes were used for the Mg targets. The Si^{28} target was prepared from transistor grade silicon. The N^{14}, O^{16}, Ne^{20} (98.1% Ne^{20}) and Ar^{40} nuclei were bombarded in a gas holder filled to about 25 cm pressure.

III. RESULTS

The reactions that were investigated are discussed separately here—Sec. IV and a previous publication[1] present the general framework upon which our spin assignments to the preferentially populated levels are based.

A. The $C^{12}(\alpha,d)N^{14}$ Reaction

This reaction has been discussed in detail in a previous publication.[4] Figure 2 shows the deuteron energy spectrum observed at 30 deg induced by 53-MeV alpha particles. The angular distribution of the highly populated level at 9.00 ± 0.05 MeV, which has been assigned a $(d_{5/2})^2_5$ configuration,[1] is shown in Fig. 3. Further, the relatively large peak that arises at an excitation of 15.1 ± 0.1 MeV is thought to have a $(d_{5/2}\ f_{7/2})_6$ configuration.[4]

B. The $N^{14}(\alpha,d)O^{16}$ Reaction

This reaction had been studied previously using the 48-MeV alpha beam of the Crocker 60-inch cyclotron.[5] Since the spin of the target nucleus is 1, three levels having $(d_{5/2})^2_5$ configurations—with spins of 4, 5, and 6—should be observed. However, only two large peaks, at 14.7 and 16.2 MeV were observed, and it was then believed[1] that the third member of the triplet was located at a higher excitation than investigated in that work.

Figure 4 shows a deuteron energy spectrum from a more recent investigation of this reaction using a 42.3-MeV alpha beam from the Berkeley 88-inch cyclotron. It is now obvious that all three members of the triplet were observed during the first investigation but that the energy resolution of the system was insufficient to separate them. The highly populated levels lie at 14.33 ± 0.10, 14.74 ± 0.10 and 16.16 ± 0.10 MeV of excitation. Figure 5 shows the angular distributions of these levels. Energy spectra were obtained at only a few angles but the shape of the angular distributions of these three levels closely resembles the shape previously observed for the angular distributions of the 14.7-MeV and 16.2-MeV levels.[1]

Specific spin assignments to these levels have not been made although a 6+ level at 16.2 MeV was recently reported by Carter et al.[6] from a $C^{12}(\alpha,\alpha)C^{12}$ study. However, they did not observe the 4+ level which appears inconsistent if the same level at 16.2 MeV was observed in both experiments. There is a 4+ level at 14.92 MeV[7] that possibly corresponds to the level we find at 14.74 MeV, but an error in our energy calibration of that amount would displace the "16.16 MeV" level to 16.34 MeV, which would no longer be in agreement with the 6+ level previously seen. On the basis of our simple model the relative population of these levels could be used to predict the specific spin assignments, since the cross section is proportional to $2J + 1$. Thus spins of 4, 6, and 5 in order of increasing excitation would be predicted because the integrated cross sections are 2.2, 3.5, and 2.9 mb, respectively (between ≈12.5 to 70 deg, c.m.). After dividing by $2J + 1$, one finds excellent agreement: 0.74, 0.81, and 0.79, supporting the above assignments.

Observation of a definite peak at about 13.1-MeV excitation in this (α,d) reaction is additional evidence for a T=0 state of O^{16} in this region.[8,9]

C. The $O^{16}(\alpha,d)F^{18}$ Reaction

Formation of a preferentially populated $(d_{5/2})^2_5$ level by this reaction has been reported.[1] This reaction was recently observed over the angular range from 11 to 50 deg using a 52-MeV alpha beam from the 88-inch cyclotron. Figure 6 shows the deuteron energy spectrum measured at 20 deg. Excited levels of F^{18} were seen at 1.10, 2.05, 3.68, 4.25, 6.12, 6.76, 7.13, 7.65, 9.44, 10.44, and 11.41 MeV. Figure 7 shows the angular distribution of the 9.44-MeV state that possibly is a $(d_{5/2}\ f_{7/2})_{6-}$ level, and also includes the angular distribution of the $(d_{5/2})^2_5$ level at 1.10 MeV. At lower bombarding energies (30-40 MeV) the 0.934-MeV level is sufficiently populated that it should be subtracted when analyzing the 5+ level,[10] but at 52 MeV its contribution appears to be negligible.

D. The $Ne^{20}(\alpha,d)Na^{22}$ Reaction

This reaction was observed with a 45-MeV alpha beam from the 88-inch cyclotron. Figure 8 shows the deuteron energy spectrum at 15 deg. The energy scale was calibrated from the $C^{12}(\alpha,d)N^{14}$ reaction taking into account the difference in target thicknesses. Table I compares the levels observed with the previously reported levels of Na^{22}.

The transition to the ground state of Na^{22} has a very small cross section. At about 0.79-MeV excitation there appears to be a doublet, but the very small population of these excited states makes identification difficult. The same problem arises in the identification of the 3.74-5.29- and 5.95-MeV levels.

If our general picture is correct, the preferentially populated state at 1.53 MeV is the $(d_{5/2})^2_5$ level; the strongly forward peaked angular distribution of this level is shown in Fig. 9. Temmer and Heydenburg[12] previously observed the $Ne^{20}(He^3,p)Na^{22}$ reaction which should also populate the $(d_{5/2})^2_5$ level strongly. However the available bombarding energy was only 3.5 MeV, thus making any relative population comparisons meaningless. The momentum transfer at 3.5 MeV is considerably less than 4 which would strongly inhibit the formation of the 5+ state, and they, in fact, observe only a very small peak at 1.54-MeV excitation. Formation of the 1.53-MeV level by the $Mg^{24}(d,\alpha)Na^{22}$ reaction[13] is not in conflict with the $(d_{5/2})^2_5$ assignment, since the $d_{5/2}$ shell is populated in Mg^{24}. The strongly populated level at 7.46 MeV, whose angular distribution is also shown in Fig. 9, probably arises from a $(d_{5/2}\ f_{7/2})_6$ configuration.

E. The $Mg^{24}(\alpha,d)Al^{26}$ and $Mg^{26}(\alpha,d)Al^{28}$ Reactions

Although the Al^{26} nucleus has been well studied (Ref. 11 and references therein) the formation of this nucleus by the (α,d) reaction has not been investigated previously. Figures 10 and 11 show the deuteron energy spectrum recorded at 12 and 50 deg, respectively, using a 50.8-MeV alpha beam. Table II presents a list of the levels observed, and Figs. 12 and 13 show the angular distributions of most of these levels.

Since the Mg^{24} nucleus already contains four protons and four neutrons in the $d_{5/2}$ shell, the 5+ ground state of Al^{26} probably has a $(d_{5/2})^2_5$ configuration. Figure 12 includes the angular distribution corresponding to this transition, whose cross section is 1.06 mb over the angular range from 13.6 to 66.8 deg (c.m.).

The level at 6.95 MeV, whose angular distribution also appears in Fig. 12, dominates the energy spectrum. There is no previous spin assignment for this level but our data indicate that it arises from a $(d_{5/2}\ f_{7/2})_6$ configuration. This transition has a cross section of 1.85 mb between 13.9 and 67.8 deg (c.m.).

The excitation region above 8.17 MeV has not been investigated previously. At 8.27-MeV excitation a relatively large peak is observed. This level possibly arises from a $(f_{7/2})^2_7$ configuration, and will be given that assignment here. Figure 11 shows several other peaks that stand out clearly above the background in the excitation region between about 8 and 12 MeV; however, at smaller angles (see Fig. 10) the peak at 8.27 MeV dominates the spectrum in this region. Although the excitation region investigated extended up to about 25 MeV no well-defined levels above 12 MeV were observed. Al^{26*} ($E^* > 11.4$ MeV) can break-up into Mg^{24} and a deuteron.

A similar $(f_{7/2})^2_7$ level should be preferentially populated in the $Mg^{26}(\alpha,d)Al^{28}$ reaction but no level having a large $(d_{5/2})^2_5$ component should be observed. Furthermore, the probability of populating a $(d_{5/2}\ f_{7/2})_{6^-}$ level should be decreased since only the proton can enter the $d_{5/2}$ shell. Figure 14 shows a deuteron energy spectrum from the $Mg^{26}(\alpha,d)Al^{28}$ reaction at 40 deg. Although the counter system was not sufficiently thick to stop deuterons corresponding to the ground state transition at small angles, thus making a precise analysis of the low excitation region difficult, no preferentially populated levels were observed in this region. The level at 9.80 ± 0.05 MeV, whose angular distribution is shown in Fig. 15, clearly dominates the spectrum,

consequently, this level is assigned a $(f_{7/2})^2_7$ configuration. This transition has a cross section of 0.593 mb between 13.7 and 67.2 deg (c.m.). No peak of sufficient size that we would want to associate it with a $(d_{5/2}\ f_{7/2})_{6-}$ level was observed—such a level would be expected to fall at about 7.5 MeV (see Sec. IV).

F. The $Si^{28}(\alpha,d)P^{30}$ Reaction

Figure 16 shows the deuteron energy spectrum at 20 deg using a 50.8-MeV alpha beam. A rather large C^{12} and O^{16} impurity was present in the target—peaks corresponding to both the 9.00-MeV level of N^{14} and the 1.10-MeV level of F^{18} were larger than any peaks corresponding to P^{30} levels. Identification of these impurity levels was done kinematically.

Table III compares the levels observed with the previously reported levels of P^{30}. Since the $d_{5/2}$ shell is full in Si^{28}, only one preferentially populated level should be observed in this reaction, and only one is observed—at 7.03 MeV. Thus this level probably has a $(f_{7/2})^2_7$ configuration. The angular distribution of this transition, which has a cross section of 2.23 mb between 13.6 and 55.9 deg (c.m.), is shown in Fig. 17. If two highly populated levels had been observed, we would have been tempted to give a $(d_{3/2}\ f_{7/2})_{5-}$ assignment to the one at lower excitation; however, only one large peak was observed in this reaction, and in the $Mg^{26}(\alpha,d)Al^{28}$ reaction. Since levels having a $(f_{7/2})^2_7$ configuration appear to be highly populated and a $(f_{7/2})^2_7$ level at 7.03 MeV is consistent with other data (see Sec. IV), the cross section for (α,d) transitions to $(d_{3/2}\ f_{7/2})_{5-}$ levels apparently is not large.

G. The $Ca^{40}(\alpha,d)Sc^{42}$ Reaction

This reaction was first observed during the last days of the 60-inch cyclotron, but a more complete investigation was carried out with a 50-MeV alpha beam from the 88-inch cyclotron. Figure 18 shows the deuteron energy spectrum at 40 deg. The presence of the 1.10-MeV level of F^{18}, arising from an oxygen impurity, provided additional points for the energy scale.

Figure 19 compares the Sc^{42} levels observed with the levels identified in previous (He^3,p) investigations.[14,15,16] Unfortunately these different investigations do not agree very well with one another; the excitation values listed are the ones that appear to be generally consistent with the energy-level spacings (although not absolute values) of a recent $K^{39}(\alpha,n)Sc^{42}$ investigation.[17] The low-lying levels identified in the $Ca^{40}(t,p)Ca^{42}$ reaction[18] are also included for a comparison of the analog states. Such comparisons are enlightening because of the selection rules involved and because most of the low-lying levels of Sc^{42} and Ca^{42} should arise from coupling two $f_{7/2}$ nucleons to the Ca^{40} core.[19,20] In the (He^3,p) reaction the two nucleons are captured into the $f_{7/2}$ shell in either the isospin singlet or triplet state, thus allowing any value of angular momentum between 0 and 7. However in the (α,d) reaction these two nucleons must be captured in the isospin singlet state, and consequently only odd spin states are allowed. Conversely, since the two neutrons captured in the $f_{7/2}$ shell in the (t,p) reaction must be in the isospin triplet state, only even spin states are allowed.

The levels observed at 0, 1.51, 1.92, 2.4, and 2.75 MeV in the (He^3,p) reaction are probably the analog states of Ca^{42}. Therefore these levels have the spin assignments given in Fig. 19, and of course are T=1 levels. None of these levels should be made by the (α,d) reaction and, except for a possible uncertainty because the large peak at 1.43 MeV in the (α,d) spectra would obscure a small peak corresponding to the 1.51-MeV level, none of these levels were observed in our work. The peak at about 1.51-MeV excitation, which dominates the (He^3,p) spectra,[15] probably corresponds to two levels; the analog state of Ca^{42} and the level observed in the (α,d) reaction. Additional evidence for such an explanation comes from a comparison of peak widths in this (He^3,p) spectrum; the peak at 1.51 MeV is definitely broader than the other peaks.

In the (α,d) reaction the peak at about 0.60-MeV excitation dominates the spectrum. A level at this excitation has already been associated with a spin of 6 or 7 (probably 7) from positon decay studies.[21,22] This is in agreement with the $(f_{7/2})^2_{7+}$ assignment made here on the basis of the preferential population. Nelson et al.[17] erroneously reported that this high spin state had not been observed prior to their (α,n) investigation. They apparently were misled because of the discrepancy between their observed excitation of 0.526 MeV and our reported value.[23] This discrepancy arises through their inability to determine the mass excess of Sc^{42} correctly using the (α,n) reaction.[24] They report a mass excess about 120 keV larger than the value obtained by the (He^3,p) and (p,n) experiments. If their 7+ level is aligned with our 7+ level, their high spin state at 1.34 MeV corresponds to our (5+)

level at 1.43 MeV, and their 1.42-MeV level probably corresponds to the 2+ level at 1.51 MeV. Thus it appears that there are only two levels around 1.4 to 1.5-MeV excitation—this would account for the failure to observe three levels in this region in the (α,n) investigation.[17] The 5+ level probably is the $(f_{7/2})^2$ configuration that was assumed to fall at 1.958 MeV.[20] This energy-level scheme for the low-lying states of Sc^{42} also contradicts the rather naive interpretation that the large peak we see at 1.43-MeV excitation arises from an isospin impurity.[15] Recently Ginocchio[25] reported incorrectly that the level at 1.43 MeV was weakly excited in our work, and was the isobaric analog of the $J = 2+$, $T = 1$, state in Ca^{42}.

Figure 20 presents the angular distributions of the 0.60- and 1.43-MeV levels, whose cross sections between 13.7 and 64.2 deg (c.m.) are 4.3 and 1.5 mb, respectively. At about 2.25 MeV a small peak which could correspond to the tentative $(f_{7/2})^2_3$ level[20] was observed.

H. The $Ar^{40}(\alpha,d)K^{42}$ Reaction

A very brief investigation of this reaction was carried out with a 44-MeV alpha beam in an attempt to identify the $(f_{7/2})^2_7$ level in K^{42}. The deuteron energy spectrum, shown in Fig. 21, was dominated by a highly populated level at 1.87 MeV, whose cross section was 1.6 mb between 11.6 and 53.8 deg (c.m.).

IV. DISCUSSION

The preferential excitation of certain nuclear levels in (α,d) reactions on light elements has been reported in a previous publication.[1] These preferentially populated levels were reported to have $(d_{5/2})^2_5$ configurations. Such an assignment is strongly favored by the kinematics of the reaction. The strongest transfer reactions should be those involving minimal disturbance of the target core and a simple delivery of the two nucleons to the surface of this core. For alpha energies of about 48 MeV, involved in all of these measurements, the angular momentum transferred in a surface interaction is about 4 to 6 $\hbar$ when the deuteron escapes at 0 deg. Consequently transitions to levels formed by capturing both of the stripped nucleons into shells having orbital angular momentum values of 2 or 3 $\hbar$ should be enhanced. Formation of a $(d_{5/2})^2$ level requires that l_n and l_p both be equal to 2 $\hbar$. A value of 4 $\hbar$ for the sum of l_n and l_p permits the maximum overlap between the radial wave functions of the two nucleons so that their final state is as similar as possible to their initial state. Ignoring spin-flipping interactions, the captured nucleons will retain their initial triplet configuration. Thus states with a strong ^3G amplitude will be favored at small angles. Likewise states whose configurations have large ^3H and ^3I amplitudes should also be preferentially populated. That this is a necessary—but not always a sufficient—requirement to guarantee preferential population has been demonstrated.[26] Table IV lists the amplitudes of the possible L-S components of $(d_{5/2})^2$, $(d_{3/2}\ d_{5/2})$, $(d_{3/2})^2$, $(d_{5/2}\ f_{7/2})$, $(d_{3/2}\ f_{7/2})$, and $(f_{7/2})^2$ configurations. We see that the $(d_{5/2})^2_5$, $(d_{5/2}\ f_{7/2})_6$, and $(f_{7/2})^2_7$ configurations

are likely candidates for levels preferentially populated by the (α,d) reaction, although the $(d_{3/2})^2_3$, $(d_{3/2}\ d_{5/2})_4$, and $(d_{3/2}\ f_{7/2})_5$ configurations must also be considered. Although configurations of two nucleons in the same shell have more spatial overlap, transitions to configurations of two nucleons in different shells get additional enhancement because of the greater possible interchange and because more holes are available.

In the previous investigation,[1] the first evidence that all the strongly populated levels might be of the same $(d_{5/2})^2_5$ configuration was obtained when the Q values for their formation were plotted as a function of the mass number of the product nucleus. As Fig. 22 illustrates, the (negative) Q values decrease in a regular way with increasing A. This relationship has now been extended to higher mass numbers by the addition of the 1.53-MeV level of Na^{22} and the ground state of Al^{26}. Figure 22 also includes the Q values for the formation of the other preferentially populated levels reported herein. These points fall into what appears to be two groups, both of which resemble the behavior of the $(d_{5/2})^2_5$ points. This information was very useful in making the $(d_{5/2}\ f_{7/2})_6$, and $(f_{7/2})^2_7$ assignments given in this paper. The positions of these levels are reasonably consistent with shell-model calculations. True[27] predicts that the $(d_{5/2})^2_{5+}$, $(d_{5/2}\ f_{7/2})_{6-}$, $(d_{3/2}\ f_{7/2})_{5-}$, and $(f_{7/2})^2_{7+}$ levels should lie at about 9-, 15-, 19-, and 24-MeV excitation in N^{14}, respectively. We found preferentially populated levels at 9.00 and 15.1 MeV in N^{14} and have given them $(d_{5/2})^2_{5+}$ and $(d_{5/2}\ f_{7/2})_{6-}$ assignments. Unfortunately, equally reliable calculations cannot be made throughout the mass region studied here because of lack of knowledge of

single-particle level positions. (And this study included a region of highly distorted nuclei where the concept of good single-particle levels is not applicable.) However, simple calculations based on single particle level positions in O^{17} (Ref. 28) and on the first reported 7/2- level in the higher A nuclei,[11] where available, are in fairly good agreement (usually within 1 MeV) with the assignments given here. Furthermore, the position of the previously assigned [21,22] 7+ level in Ca^{40} is in excellent agreement with where we would predict such a level on the basis of our systematics.

Preferential population of $(d_{3/2})^2_{3+}$, $(d_{3/2}\ d_{5/2})_{4+}$, and $(d_{3/2}\ f_{7/2})_{5-}$ levels was not observed. If $(d_{3/2})^2_{3+}$ levels were preferentially populated, a large peak at low excitation would have been observed in the $Si^{28}(\alpha,d)P^{30}$ reaction; the $(d_{3/2})^2_{3+}$ level has been predicted at 2.73 MeV in P^{30} and was associated with the 3+ level at 2.54 MeV.[29] There was no indication whatsoever of such a peak. Observation of only one large peak in the $Mg^{26}(\alpha,d)Al^{28}$ and $Si^{28}(\alpha,d)P^{30}$ reactions, which was correlated with $(f_{7/2})^2_{7+}$ levels, is evidence against a preferential population of $(d_{3/2}\ f_{7/2})_{5-}$ levels. Why levels containing a nucleon in the $d_{3/2}$ shell are not preferentially populated is an interesting, but unanswered, question at the present time. An investigation of the (α,d) reaction on masses 30, 32, 34, and 36 would be valuable in conclusively proving if the observed preferential population of only $(f_{7/2})^2_{7+}$ levels is true throughout the latter half of the sd shell.

Describing the preferentially populated levels in terms of states of good J in deformed nuclei appears to be fairly well justified since most of the strength goes to one level; no indication of a series of peaks built on a large peak was observed. Thus it appears that even in deformed nuclei the coupling between the two captured nucleons and the target core is relatively weak.

As Fig. 23 illustrates, the angular distributions of the deuteron groups corresponding to the $(d_{5/2})^2_{5+}$ levels closely resemble one another, and they have therefore been used as an additional basis for the assignments of the preferentially populated levels. In no case is there any evidence for diffraction-like oscillations for the preferentially populated transitions, and the distributions are all strongly peaked in the forward direction. However, the angular distribution of the transition to the 5+ ground state of Al^{26}, which is not highly populated, exhibits a well-defined structure. The oscillatory angular distribution observed is not surprising since the semi-classical explanations used for the other $(d_{5/2})^2_5$ levels may not be as applicable here because of the relatively low cross section.

Figure 24 presents a plot of the summed cross sections of the $(d_{5/2})^2_{5+}$ levels, integrated over similar angular ranges ($\approx$12.5° to 70 deg, c.m.) vs the mass number of the product nucleus. A constant cross section to these states is expected when the target nuclei all have completely empty $d_{5/2}$ shells; as the $d_{5/2}$ shell is filled, the cross section should decrease. The data are in good accord with this except for the transition to the $(d_{5/2})^2_{5+}$ level in the $C^{12}(\alpha,d)N^{14}$ reaction, which has a considerably smaller cross section than the other transitions to an empty $d_{5/2}$ shell. At present we have no explanation for this reduced cross section.

Figure 25 presents the angular distributions of the transitions to the tentative $(d_{5/2}\ f_{7/2})_{6-}$ and $(f_{7/2})^2_{7+}$ levels. These angular distributions again resemble one another, and also resemble the angular

distributions of the $(d_{5/2})^2_{5+}$ levels. The structure shown by the angular distribution of the transition to the 0.60 MeV level of Sc^{42} probably arises because the observed peak corresponds to two levels (see Fig. 19) although the observed cross section should be attributed predominately to the 7+ level.

A plot of the integrated cross sections of the $(f_{7/2})^2_{7+}$ levels vs the mass number of the product nucleus illustrates that, in general, the cross section increases as the product mass increases up to Sc^{42} where the $f_{7/2}$ shell is beginning to fill. We do not have data in the mass region where the $f_{7/2}$ shell is partially full, although we expect the cross section would decrease for $A > 42$. A similar plot of the $(d_{5/2}\,f_{7/2})_{6-}$ levels is rather flat, as might be expected after observing the $(d_{5/2})^2_{5+}$ and $(f_{7/2})^2_{7+}$ cross sections as a function of mass number.

V. CONCLUSION

Although most of the $(d_{5/2}\ f_{7/2})_{6-}$ and $(f_{7/2})^2_{7+}$ assignments made herein must be considered tentative, it appears that the (α,d) reaction will prove to be a very valuable spectroscopic tool for locating certain types of two-particle states when utilized in the manner demonstrated.

ACKNOWLEDGMENTS

We are indebted to Norman K. Glendenning, William W. True, and Gerald T. Garvey for many valuable discussions. We also wish to thank Fred S. Goulding, Jack H. Elliott, and Donald A. Landis for invaluable assistance with the semi-conductor detectors and electronics, and James Haag for help in collecting the data.

Table I. Comparison of Na^{22} levels observed in this experiment with those previously reported.[a]

Levels observed (MeV)	Previously reported levels		Intensity[b]
	Energy (MeV)	Jπ	
0	0	3+	0.15
	0.587	1+	
	0.660	0+	
0.79[c] ± 0.20	0.892	(1)+	Very weak
1.53 ± 0.05	1.532	(5+)[d]	2.06
	1.942		
	1.95		
	1.988		
	2.217		
	2.574		
2.98 ± 0.10	2.973		0.54
	3.065		
	3.527		
3.74 ± 0.10	3.71		Weak
	3.949		
	4.07		
	4.32		
	4.36		
	4.47		
	4.53		
4.68 ± 0.10	4.60		Fairly Strong
	4.73		
	4.77		

Table I. Continued.

Levels observed (MeV)	Previously reported levels		Intensity[b]
	Energy (MeV)	Jπ	
5.29 ± 0.20			Weak
5.95 ± 0.10			Weak
6.62 ± 0.10			0.51
7.46 ± 0.07	7.474	(6-)[d]	1.07
	7.57		
	7.71		
7.85 ± 0.10	7.81		
	7.90		
	7.98		
	8.04		

[a]Reference 11.

[b]The numbers are the cross section in mb integrated over the angular range from 10 to 52.5 deg (lab).

[c]Unresolved doublet.

[d]Assigned by this work.

Table II. Comparison of Al^{26} levels observed in this experiment with those previously reported.[a]

Levels observed (Mev)	Previously reported levels		Intensity[b]
	Energy (MeV)	Jπ	
0	0	5+	1.06 mb
	0.229	0+	
0.42 ± 0.03	0.418	3+	0.37 mb
1.05 ± 0.05	1.059	1+	Very weak
	1.760	2+	
1.85 ± 0.03	1.852	(2,3)+	Weak
	2.072	2+	
2.40 ± 0.10	2.367	2-,3-	Weak
3.00 ± 0.05	----------		Fairly strong
3.60 ± 0.05	The level density is too		Weak
4.69 ± 0.05	high to allow any useful		Weak
5.50 ± 0.05	comparisons to be made in		0.72 mb
6.59 ± 0.05	this region		0.95 mb
6.95 ± 0.05			1.85 mb
7.60 ± 0.5	----------		Fairly strong
8.27 ± 0.05	This excitation region was		1.22 mb
8.93 ± 0.07	not investigated previously		Fairly strong
9.84 ± 0.07			Fairly strong
10.71 ± 0.10			Fairly strong
11.00 ± 0.10			Weak
11.87 ± 0.10	----------		Strong

[a] Reference 11.

[b] Range of integration: 12 to 60 deg (lab).

Table III. Comparison of P^{30} levels observed in this experiment with those previously reported.[a]

Levels observed (MeV)	Previously reported levels		Intensity
	Energy (MeV)	J π T	
(0)	0	1 + 0	Very weak
	0.684	0 + 1	
	0.705	1 + 0	
	1.451	2 +	
1.97	1.972	3 +	Weak
	2.538	(2,3)+	
	2.723	2 +	
	2.839		
	2.937	2 + 1	
3.05	3.018	1 +	
	3.734		
	3.836		
4.10	↑		Fairly strong
4.80	The level density is too high to allow any useful comparisons to be made in this region.		medium
7.03			2.23 mb
9.29			medium
	↓		

[a]Reference 11.

Table IV. j-j wave functions.

Configuration	J	L-S components
$(d_{5/2})^2_J$	5	$1.00\ {}^3G$
	4	$\sqrt{\frac{4}{5}}\ {}^3F + \sqrt{\frac{1}{5}}\ {}^1G$
	3	$-\sqrt{\frac{4}{175}}\ {}^3G + \sqrt{\frac{108}{175}}\ {}^3D + \sqrt{\frac{63}{175}}\ {}^1F$
	2	$-\sqrt{\frac{9}{125}}\ {}^3F + \sqrt{\frac{56}{125}}\ {}^3P + \sqrt{\frac{60}{125}}\ {}^1D$
	1	$-\sqrt{\frac{4}{25}}\ {}^3D + \sqrt{\frac{7}{25}}\ {}^3S + \sqrt{\frac{14}{25}}\ {}^1P$
	0	$-\sqrt{\frac{2}{5}}\ {}^3P + \sqrt{\frac{3}{5}}\ {}^1S$
$(d_{3/2}\ f_{5/2})_J$	4	$\sqrt{\frac{5}{10}}\ {}^3G + \sqrt{\frac{1}{10}}\ {}^3F + \sqrt{\frac{4}{10}}\ {}^1G$
	3	$\sqrt{\frac{27}{350}}\ {}^3G + \sqrt{\frac{64}{350}}\ {}^3D + \sqrt{\frac{175}{350}}\ {}^3F + \sqrt{\frac{84}{350}}\ {}^1F$
	2	$\sqrt{\frac{32}{250}}\ {}^3F + \sqrt{\frac{125}{250}}\ {}^3D + \sqrt{\frac{63}{250}}\ {}^3P + \sqrt{\frac{30}{250}}\ {}^1D$
	1	$\sqrt{\frac{21}{150}}\ {}^3D + \sqrt{\frac{75}{150}}\ {}^3P + \sqrt{\frac{48}{150}}\ {}^3S + \sqrt{\frac{6}{150}}\ {}^1P$
$(d_{3/2})^2_J$	3	$\sqrt{\frac{144}{175}}\ {}^3G - \sqrt{\frac{3}{175}}\ {}^3D + \sqrt{\frac{28}{175}}\ {}^1F$
	2	$\sqrt{\frac{84}{125}}\ {}^3F - \sqrt{\frac{6}{125}}\ {}^3P + \sqrt{\frac{35}{125}}\ {}^1D$
	1	$\sqrt{\frac{14}{25}}\ {}^3D - \sqrt{\frac{2}{25}}\ {}^3S + \sqrt{\frac{9}{25}}\ {}^1P$
	0	$\sqrt{\frac{3}{5}}\ {}^3P + \sqrt{\frac{2}{5}}\ {}^1S$

Table IV. (Cont)

Configuration	J	L-S components
$(d_{5/2}\ f_{7/2})_J$	6	$1.00\ {}^3H$
	5	$-\sqrt{\frac{1}{175}}\ {}^3H + \sqrt{\frac{144}{175}}\ {}^3G + \sqrt{\frac{30}{175}}\ {}^1H$
	4	$-\sqrt{\frac{32}{2100}}\ {}^3H + \sqrt{\frac{33}{2100}}\ {}^3G + \sqrt{\frac{1375}{2100}}\ {}^3F + \sqrt{\frac{660}{2100}}\ {}^1G$
	3	$-\sqrt{\frac{9}{196}}\ {}^3G - \sqrt{\frac{7}{196}}\ {}^1F + \sqrt{\frac{96}{196}}\ {}^3D + \sqrt{\frac{84}{196}}\ {}^1F$
	2	$-\sqrt{\frac{16}{175}}\ {}^3F - \sqrt{\frac{15}{175}}\ {}^3D + \sqrt{\frac{54}{175}}\ {}^3P + \sqrt{\frac{90}{175}}\ {}^1D$
	1	$-\sqrt{\frac{1}{7}}\ {}^3D - \sqrt{\frac{2}{7}}\ {}^3P + \sqrt{\frac{4}{7}}\ {}^1P$
$(d_{3/2}\ f_{7/2})_J$	5	$\sqrt{\frac{12}{25}}\ {}^3H + \sqrt{\frac{3}{25}}\ {}^3G + \sqrt{\frac{10}{25}}\ {}^1H$
	4	$\sqrt{\frac{22}{525}}\ {}^3H + \sqrt{\frac{243}{525}}\ {}^3G + \sqrt{\frac{125}{525}}\ {}^3F + \sqrt{\frac{135}{525}}\ {}^1G$
	3	$\sqrt{\frac{3}{49}}\ {}^3G + \sqrt{\frac{21}{49}}\ {}^3F + \sqrt{\frac{18}{49}}\ {}^3D + \sqrt{\frac{7}{49}}\ {}^1F$
	2	$\sqrt{\frac{9}{175}}\ {}^3F + \sqrt{\frac{60}{175}}\ {}^3D + \sqrt{\frac{96}{175}}\ {}^3P + \sqrt{\frac{10}{175}}\ {}^1D$

Table IV. (Cont)

Configuration	J	L-S components
$(f_{7/2})^2_J$	7	$1.00\ {}^3I$
	6	$\sqrt{\frac{42}{49}}\ {}^3H + \sqrt{\frac{7}{49}}\ {}^1I$
	5	$-\sqrt{\frac{6}{539}}\ {}^3I + \sqrt{\frac{390}{539}}\ {}^3G + \sqrt{\frac{143}{539}}\ {}^1H$
	4	$-\sqrt{\frac{5}{147}}\ {}^3H + \sqrt{\frac{88}{147}}\ {}^3F + \sqrt{\frac{54}{147}}\ {}^1G$
	3	$-\sqrt{\frac{24}{343}}\ {}^3G + \sqrt{\frac{165}{343}}\ {}^3D + \sqrt{\frac{154}{343}}\ {}^1F$
	2	$-\sqrt{\frac{6}{49}}\ {}^3F + \sqrt{\frac{18}{49}}\ {}^3P + \sqrt{\frac{25}{49}}\ {}^1D$
	1	$-\sqrt{\frac{10}{49}}\ {}^3D + \sqrt{\frac{12}{49}}\ {}^3S + \sqrt{\frac{27}{49}}\ {}^1P$
	0	$-\sqrt{\frac{3}{7}}\ {}^3P + \sqrt{\frac{4}{7}}\ {}^1S$

Configurations of two nucleons in different shells are not states of good T.

REFERENCES

*This work was done under the auspices of the U. S. Atomic Energy Commission.

†Now at the University of Montreal, Montreal, Quebec, Canada.

1. B. G. Harvey, J. Cerny, R. H. Pehl, and E. Rivet, Nucl. Phys. 39, 160 (1962).
2. B. G. Harvey, E. Rivet, A. Springer, J. R. Meriwether, W. B. Jones, J. H. Elliott, and P. Darriulat, Nucl. Phys. 52, 465 (1964).
3. F. S. Goulding, D. A. Landis, J. Cerny, and R. H. Pehl, Nucl. Instr. Methods 31, 1 (1964).
4. R. H. Pehl, E. Rivet, J. Cerny, and B. G. Harvey, Phys. Rev. 137, B114 (1965).
5. J. Cerny, B. G. Harvey, and R. H. Pehl, Nucl. Phys. 29, 120 (1962).
6. E. B. Carter, G. E. Mitchell, and R. H. Davis, Phys. Rev. 133, B1421 (1964).
7. T. Lauritsen and F. Ajzenberg-Selove, Nuclear Data Sheets, compiled by K. Way et al. (Printing and Publishing Office, National Academy of Sciences - National Research Council, Washington 25, D.C., 1962), NRC 61-5, 6.
8. G. E. Mitchell, E. B. Carter, and R. H. Davis, Phys. Rev. 133, B1434 (1964).
9. I. V. Mitchell and T. R. Ophel, Nucl. Phys. 58, 529 (1964).
10. N. Mangelson, Lawrence Radiation Laboratory, Berkeley (private communication).
11. P. M. Endt and C. Van der Leun, Nucl. Phys. 34, 1 (1962).
12. G. M. Temmer and N. P. Heydenburg, Phys. Rev. 111, 1303 (1958).

13. C. P. Browne, Nucl. Phys. 12, 662 (1959).

14. N. Sarma, MIT Progress Report May 1, 1963 (unpublished).

15. R. W. Zurmuhle, C. M. Fou, and L. W. Swenson, Bull. Am. Phys. Soc. 9, 456 (1964); and R. W. Zurmuhle (private communication).

16. D. C. Cline, H. E. Gove, and B. Čujec, Bull. Am.Phys. Soc. 10, 25 (1965).

17. J. W. Nelson, J. D. Oberholtzer, and H. S. Plendl, Nucl. Phys. 62, 434 (1965).

18. R. Middleton and D. J. Pullen, Nucl. Phys. 51, 77 (1964).

19. J. N. Ginocchio and J. B. French, Phys. Letters 7, 137 (1963).

20. J. D. McCullen, B. F. Bayman, and L. Zamick, Phys. Rev. 134, B515 (1964).

21. P. C. Rogers and G. E. Gordon, Phys. Rev. 129, 2653 (1963).

22. J. W. Nelson, H. S. Plendl, and J. D. Oberholtzer, in Proceedings of the Rutherford Jubilee International Conference, Manchester, September 1961 (Academic Press Inc., New York, 1961), p. 819; see also J. D. Oberholtzer, J. W. Nelson, and H. S. Plendl, Bull. Am. Phys. Soc. 7, 286 (1962).

23. B. G. Harvey, E. Rivet, J. Cerny, R. H. Pehl, and J. Haag, Proceedings Conf. Nuclear Spectroscopy with Direct Reactions, Chicago (March 1964) ANL Report 6848, p. 182.

24. H. S. Plendl and J. W. Nelson, Bull. Am. Phys. Soc. 10, 479 (1965).

25. J. N. Ginocchio, Nucl. Phys. 63, 449 (1965).

26. N. K. Glendenning, Phys. Rev. 137, B102 (1965).

27. W. W. True, Phys. Rev. 130, 1530 (1963) and private communication.

28. K. Yagi, Y. Nakajima, K. Katori, Y. Awaya, and M. Fijioka, Nucl. Phys. 41, 584 (1963).

29. P. W. M. Glaudemans, G. Wiechers, and P. J. Brussaard, Nucl. Phys. 56, 548 (1964).

30. C. C. Lu, Lawrence Radiation Laboratory, Berkeley, (private communication).

FIGURE CAPTIONS

Fig. 1. Particle identifier spectrum from bombardment of C^{12} with 53-MeV alpha particles at a scattering angle of 15 deg. The discriminator settings are represented by lines 1, 2, and 3.

Fig. 2. Deuteron energy spectrum from the $C^{12}(\alpha,d)N^{14}$ reaction at a scattering angle of 30 deg.

Fig. 3. Angular distribution of deuterons from formation of the 9.00-MeV level of N^{14}.

Fig. 4. Deuteron energy spectrum from the $N^{14}(\alpha,d)O^{16}$ reaction at a scattering angle of 30 deg.

Fig. 5. Angular distributions of deuterons from formation of the 14.33-, 14.74-, and 16.16-MeV levels of O^{16}.

Fig. 6. Deuteron energy spectrum from the $O^{16}(\alpha,d)F^{18}$ reaction at a scattering angle of 20 deg.

Fig. 7. Angular distributions of deuterons from formation of the 1.10- and 9.44-MeV levels of F^{18}.

Fig. 8. Deuteron energy spectrum from the $Ne^{20}(\alpha,d)Na^{22}$ reaction at a scattering angle of 15 deg.

Fig. 9. Angular distributions of deuterons from formation of the 1.53- and 7.46-MeV levels of Na^{22}.

Fig. 10. Deuteron energy spectrum from the $Mg^{24}(\alpha,d)Al^{26}$ reaction at a scattering angle of 12 deg.

Fig. 11. Deuteron energy spectrum from the $Mg^{24}(\alpha,d)Al^{26}$ reaction at a scattering angle of 50 deg.

Fig. 12. Angular distributions of deuterons from formation of the ground state, 0.42-, 1.85-, 3.00-, 5.50-, 6.95-, and 8.27-MeV levels of Al^{26}.

Fig. 13. Angular distributions of deuterons from formation of the 3.60-, 6.59-, 7.60-, 8.93-, 9.84-, 10.71-, and 11.87-MeV levels of Al^{26}.

Fig. 14. Deuteron energy spectrum from the $Mg^{26}(\alpha,d)Al^{28}$ reaction at a scattering angle of 40 deg.

Fig. 15. Angular distribution of deuterons from formation of the 9.80-MeV level of Al^{28}.

Fig. 16. Deuteron energy spectrum from the $Si^{28}(\alpha,d)P^{30}$ reaction at a scattering angle of 20 deg.

Fig. 17. Angular distribution of deuterons from formation of the 7.03-MeV level of P^{30}.

Fig. 18. Deuteron energy spectrum from the $Ca^{40}(\alpha,d)Sc^{42}$ reaction at a scattering angle of 40 deg.

Fig. 19. The energy level schemes of Ca^{42} and Sc^{42}. The dotted lines connect analog states.

Fig. 20. Angular distributions of deuterons from formation of the 0.60- and 1.43-MeV levels of Sc^{42}.

Fig. 21. Deuteron energy spectrum from the $Ar^{40}(\alpha,d)K^{42}$ reaction at a scattering angle of 20 deg.

Fig. 22. Relationship between the mass number A of the product nucleus and the Q value for the formation of the levels preferentially populated by the (α,d) reaction.

[a]This point corresponds to a highly populated level at 5.2-MeV excitation that was observed during a brief investigation of the $S^{32}(\alpha,d)Cl^{34}$ reaction using 48-MeV alpha particles from the 60-inch cyclotron.

Fig. 23. Angular distributions of the $(d_{5/2})^2_{5+}$ levels.

Fig. 24. Integrated cross sections for the transitions to the $(d_{5/2})^2_5$ levels as a function of the mass number A of the product nucleus.

The cross section for the $N^{15}(\alpha,d)O^{17}$ reaction was obtained from a recent experiment.[30]

Fig. 25. Angular distributions of the tentative $(d_{5/2}\ f_{7/2})_{6-}$ and $(f_{7/2})^2_{7+}$ levels.

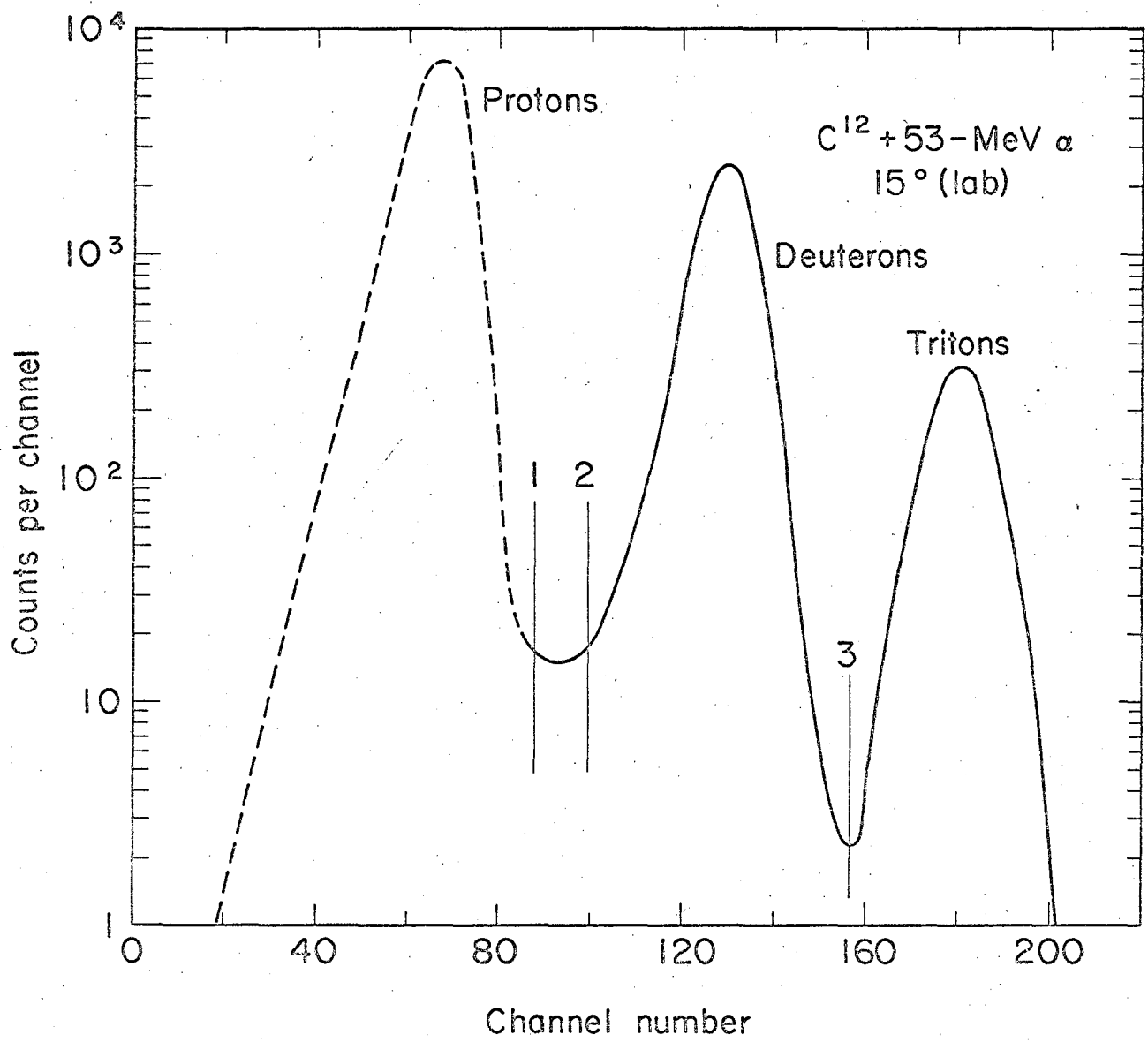

Fig. 1

MUB-3252

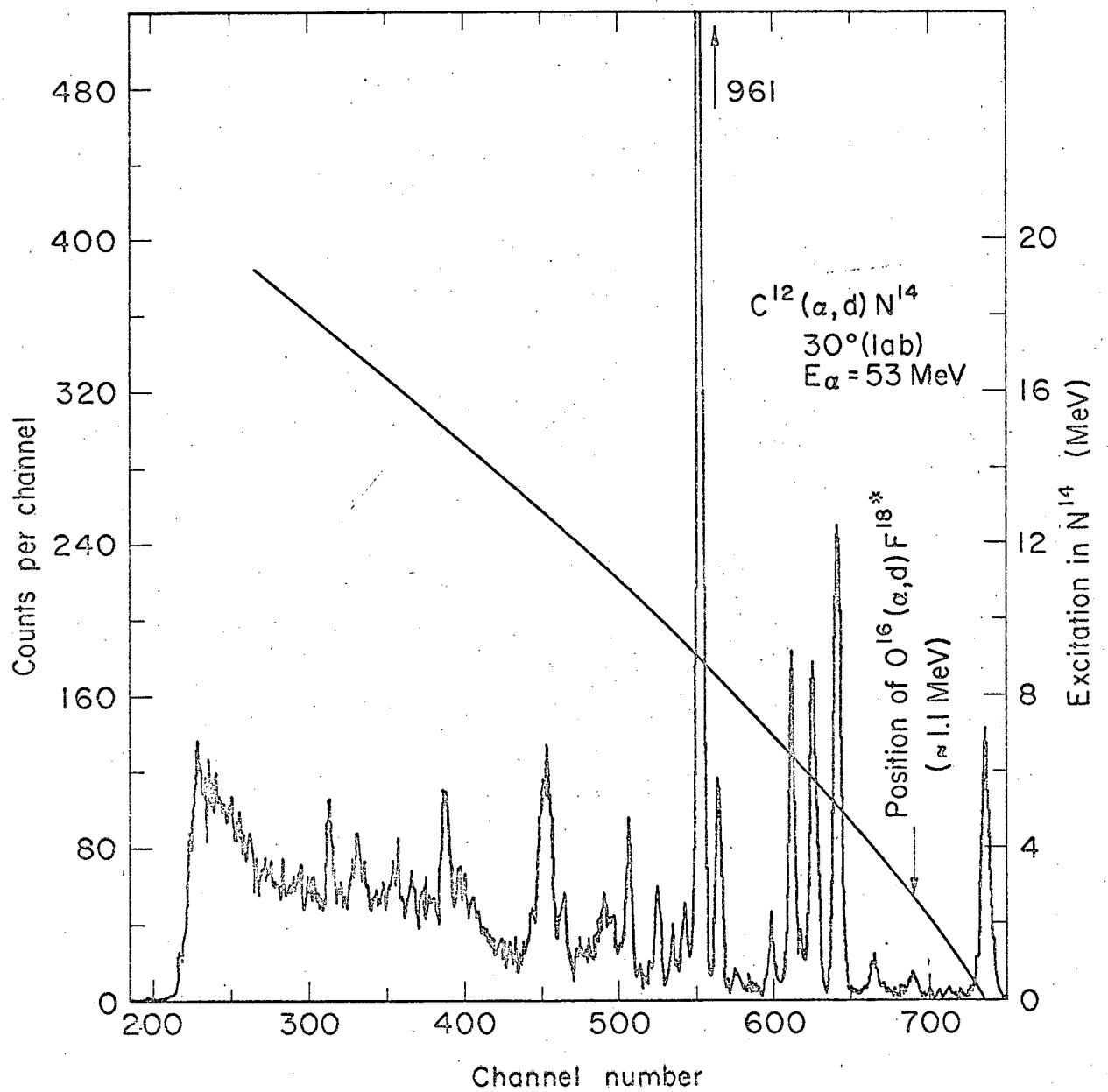

Fig. 2

MUB-3253

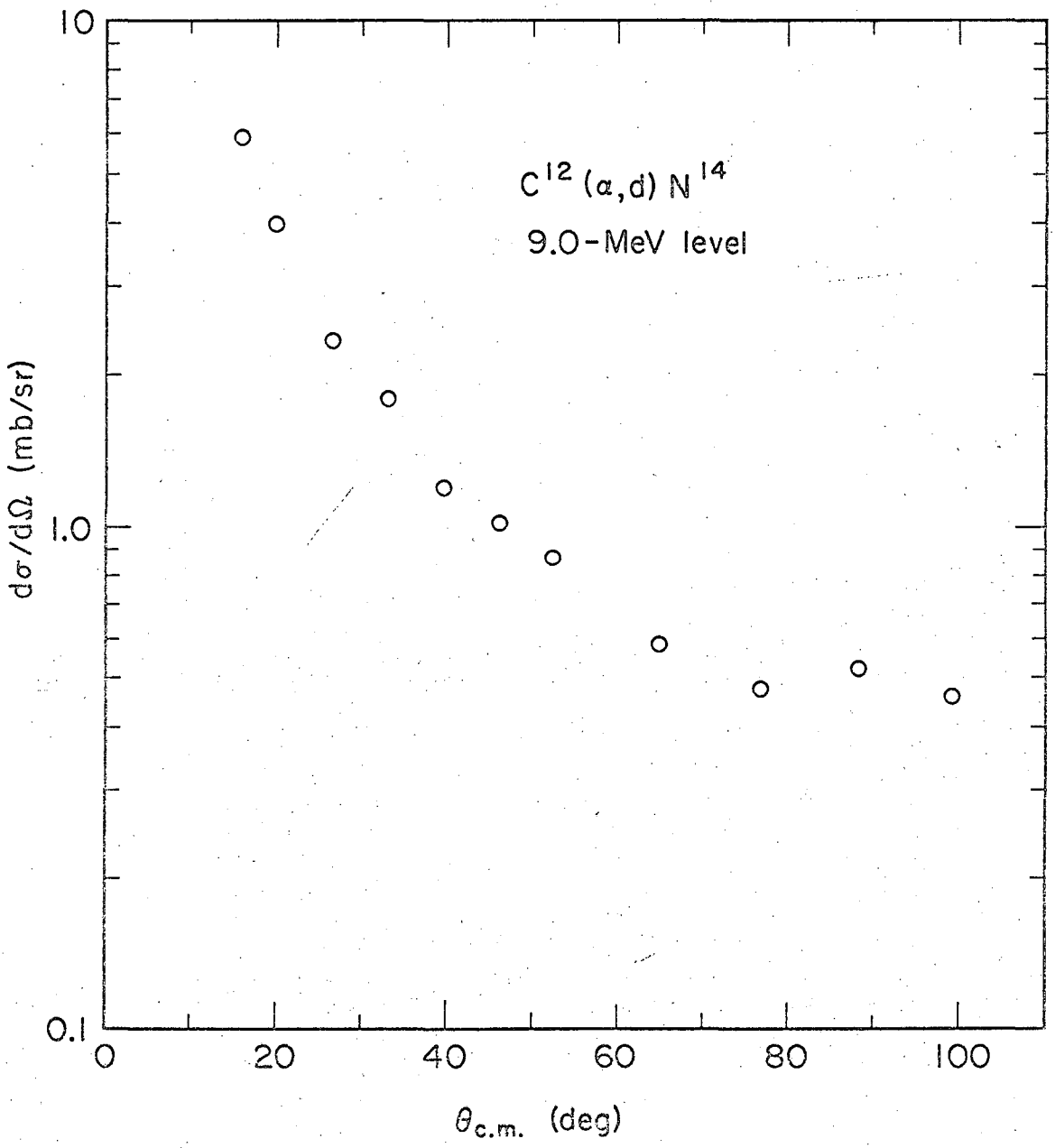

Fig. 3

MUB-3250

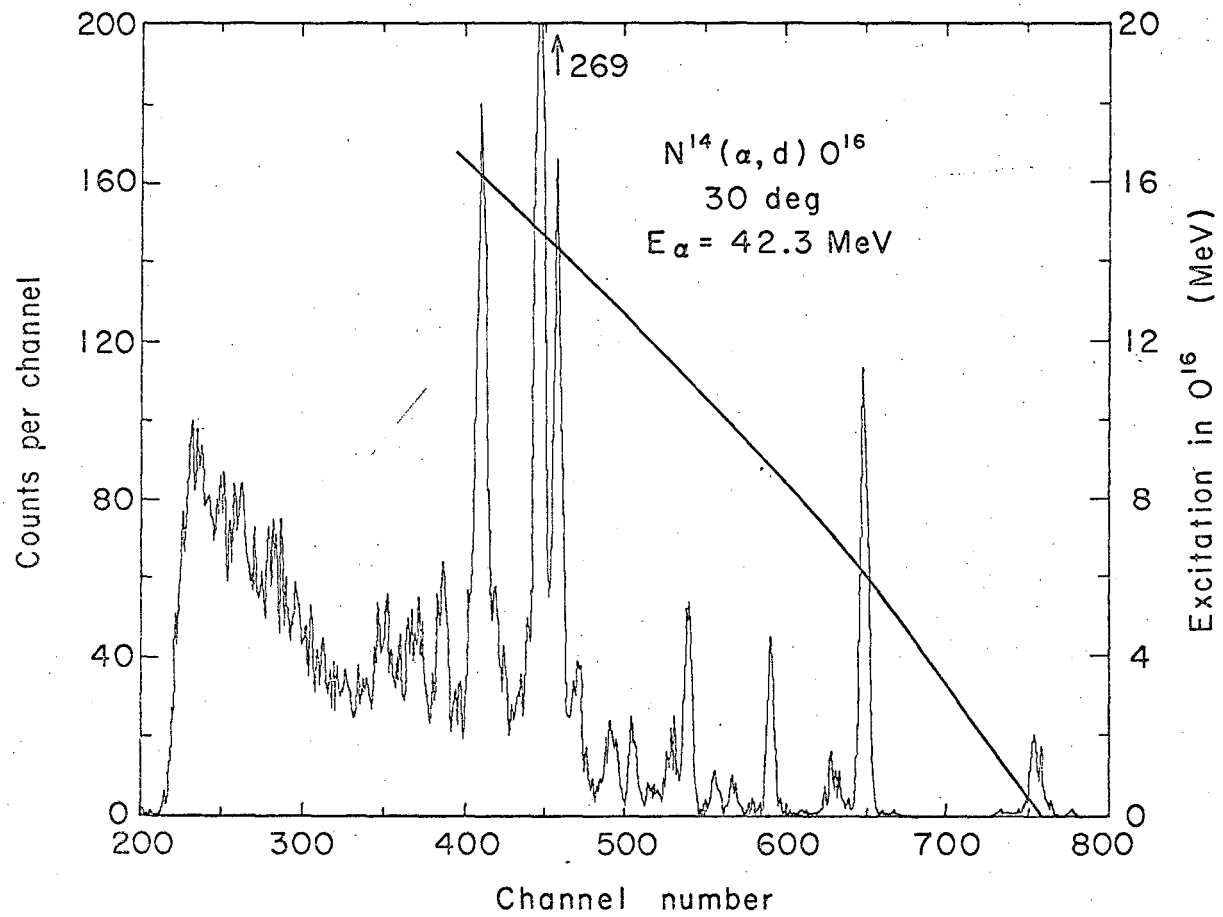

Fig. 4

MUB-6547

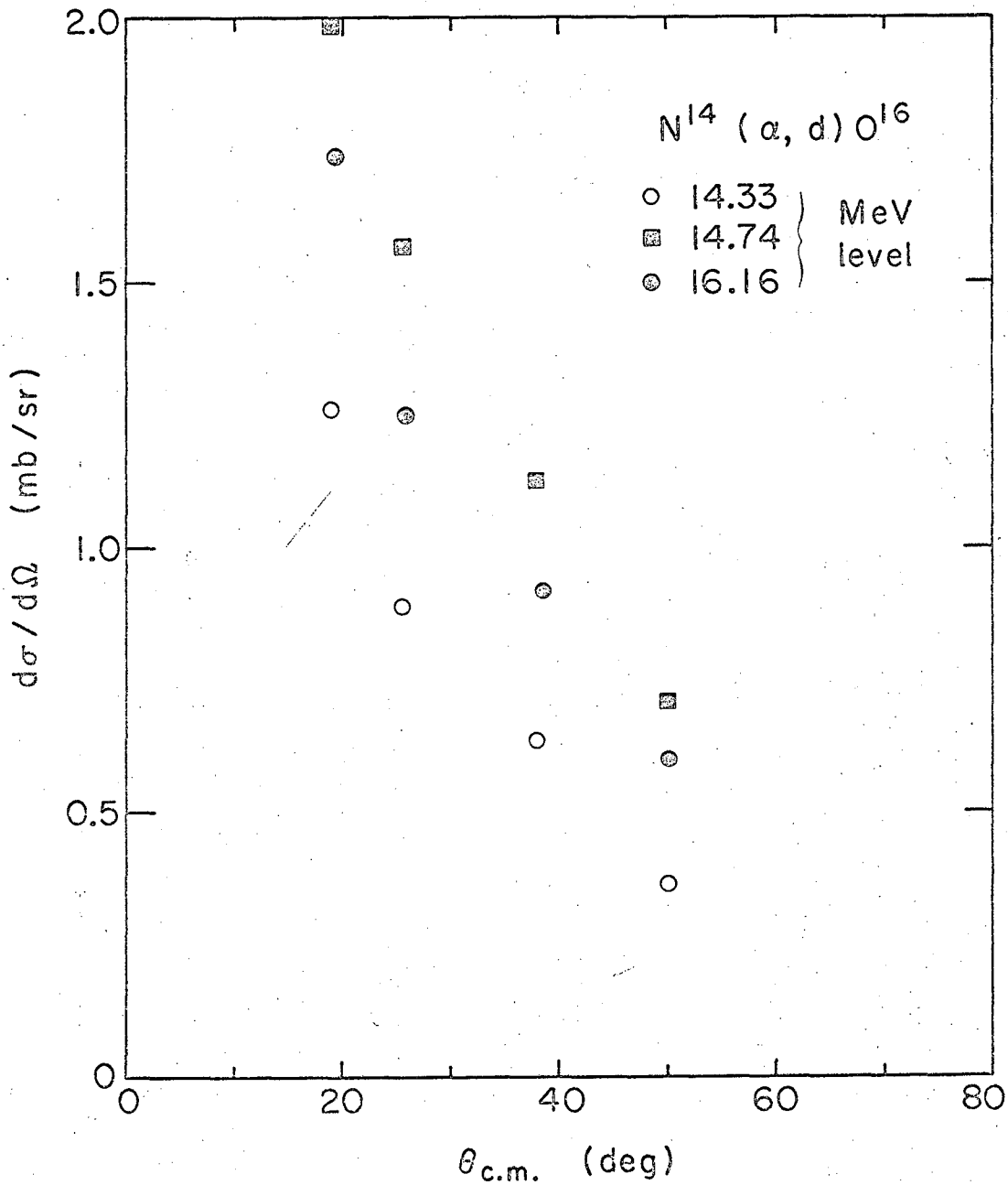

Fig. 5

MUB-6548

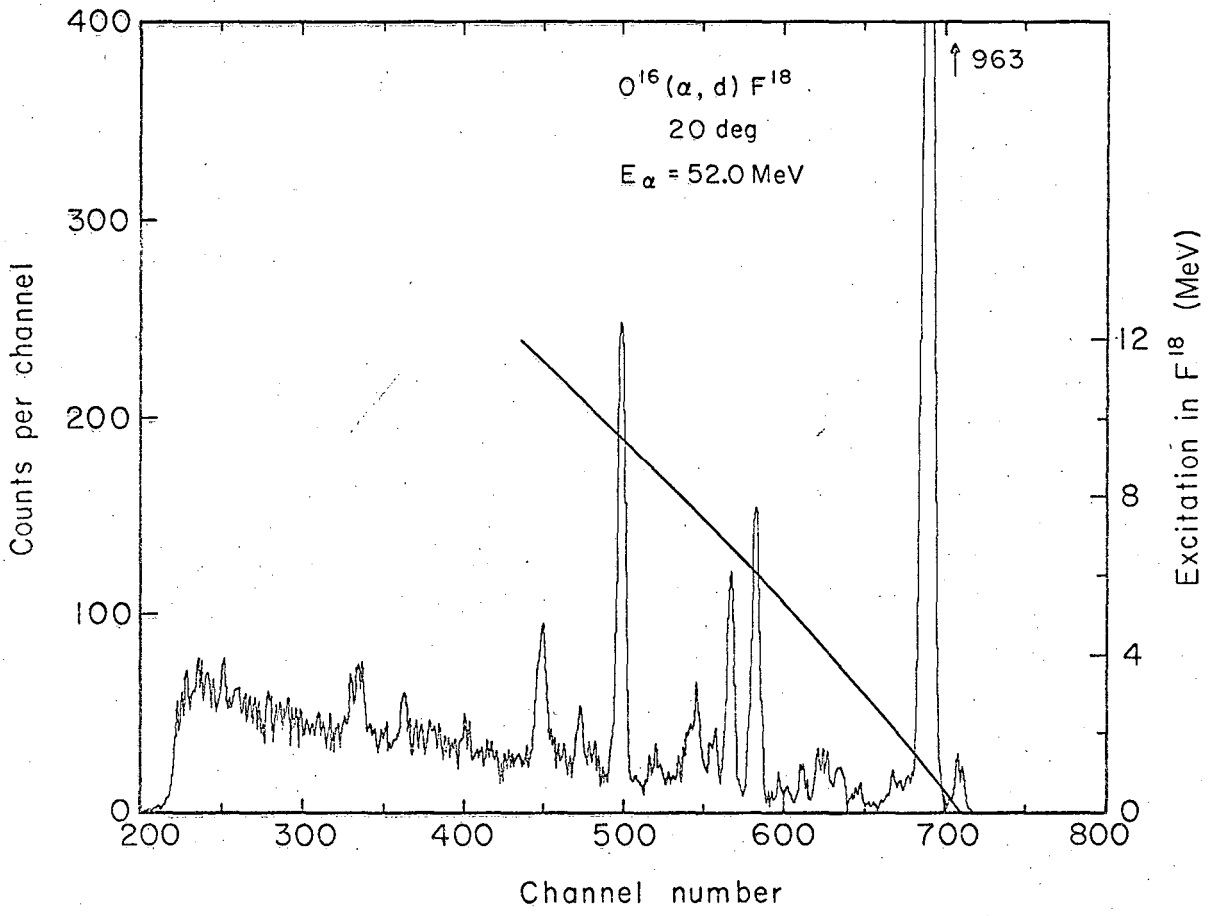

Fig. 6

MUB-6558

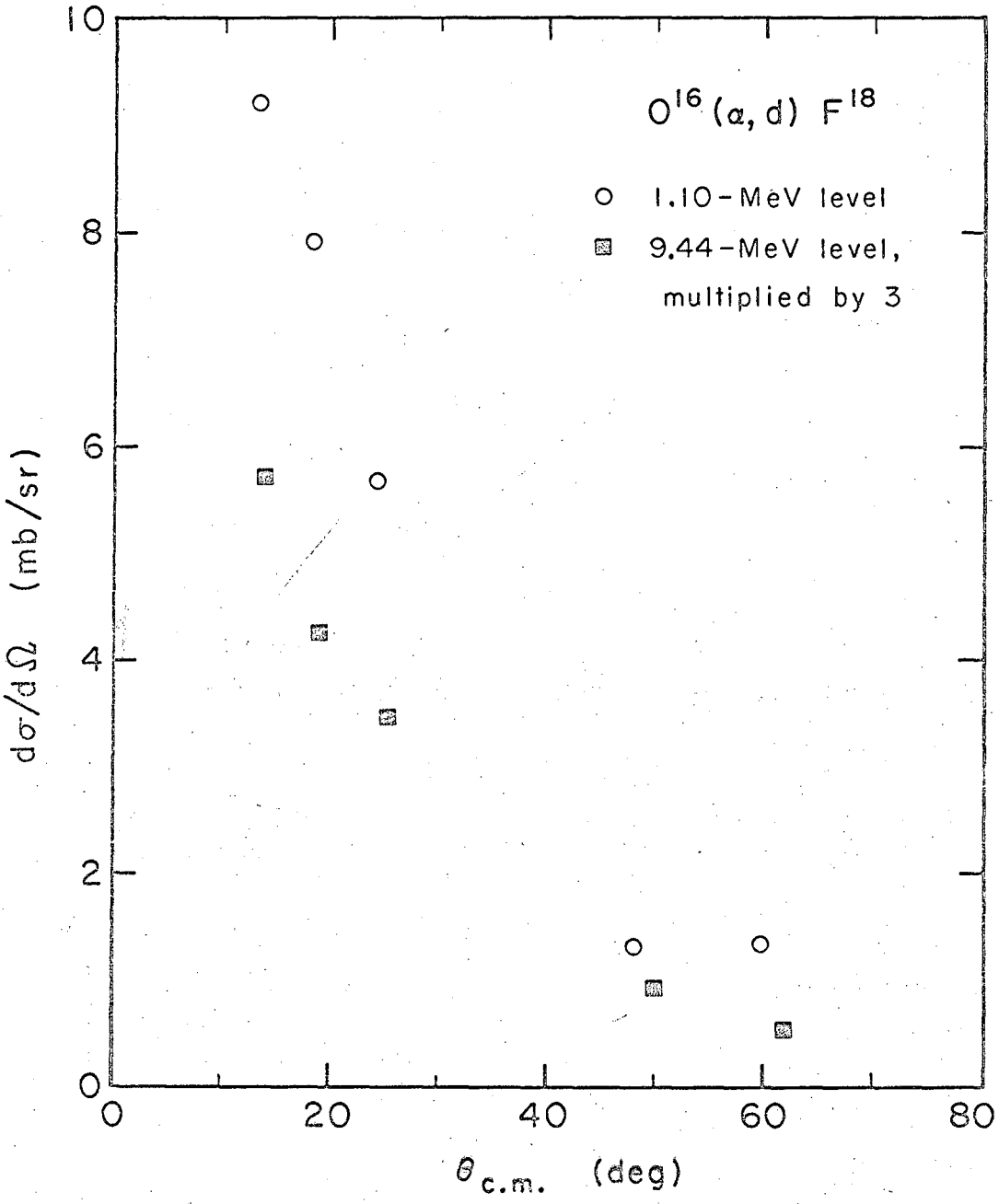

Fig. 7

MUB-6549

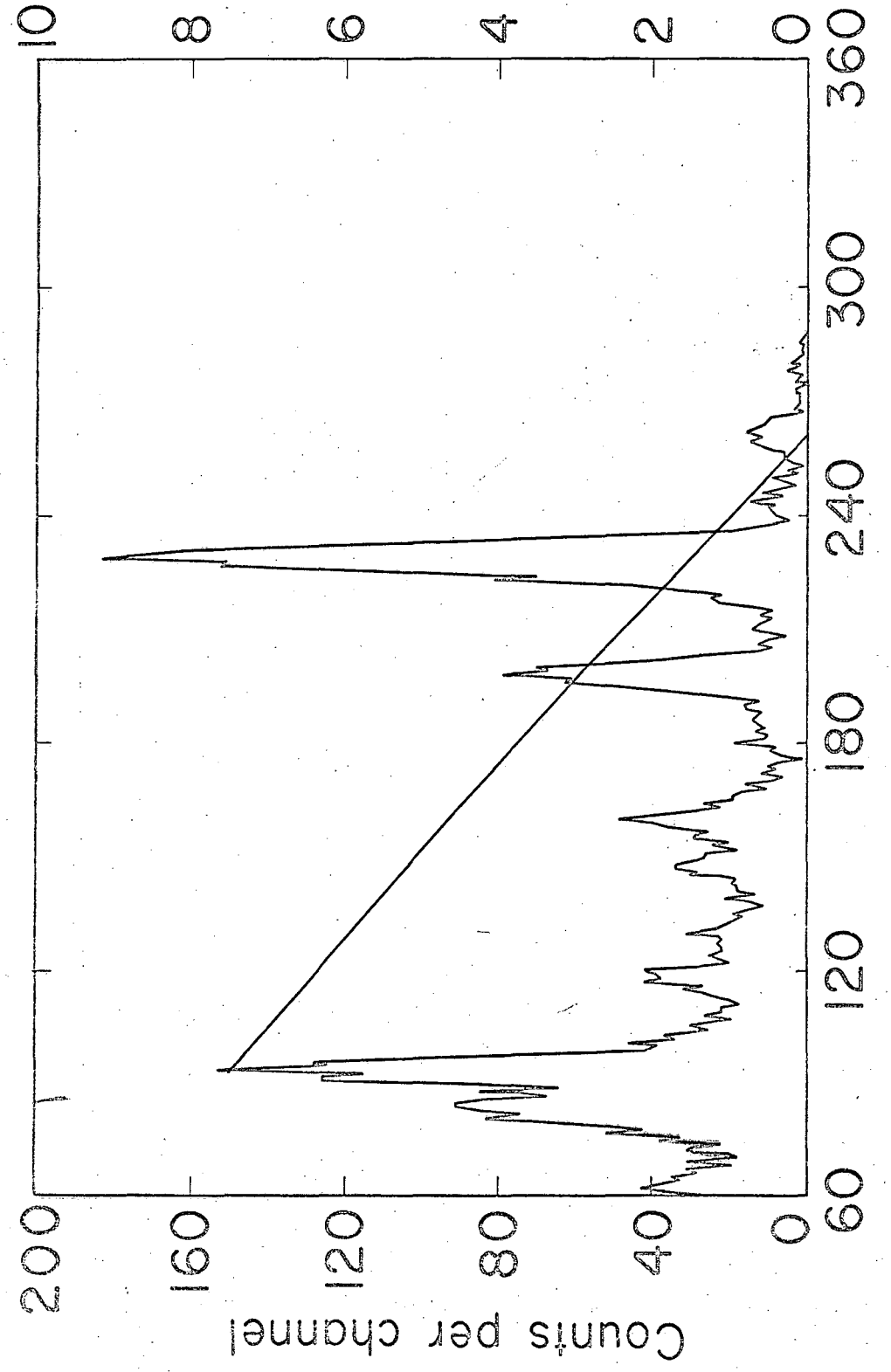

MU-33954

Fig. 8

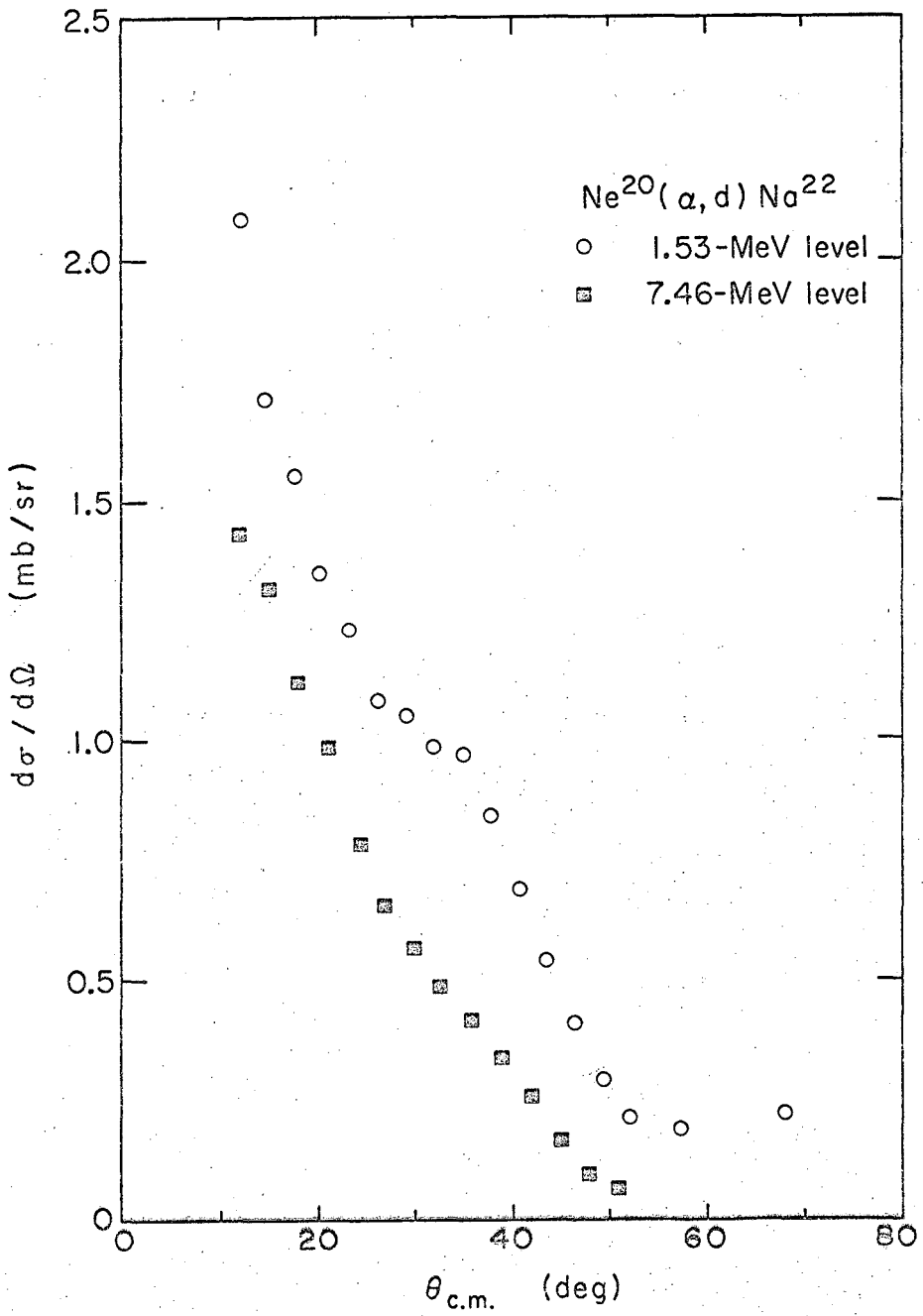

Fig. 9

MUB-6550

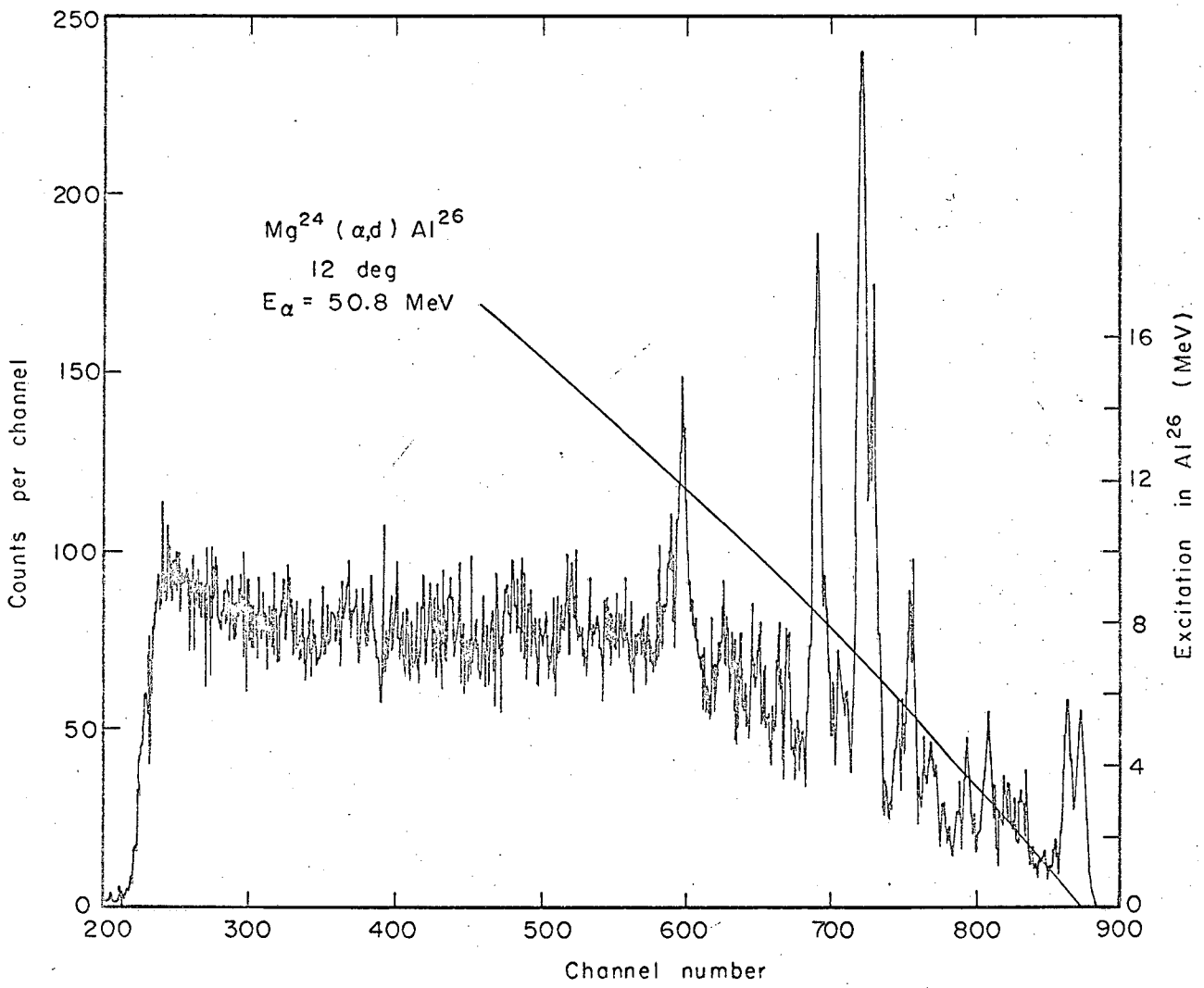

Fig. 10

MUB-6652

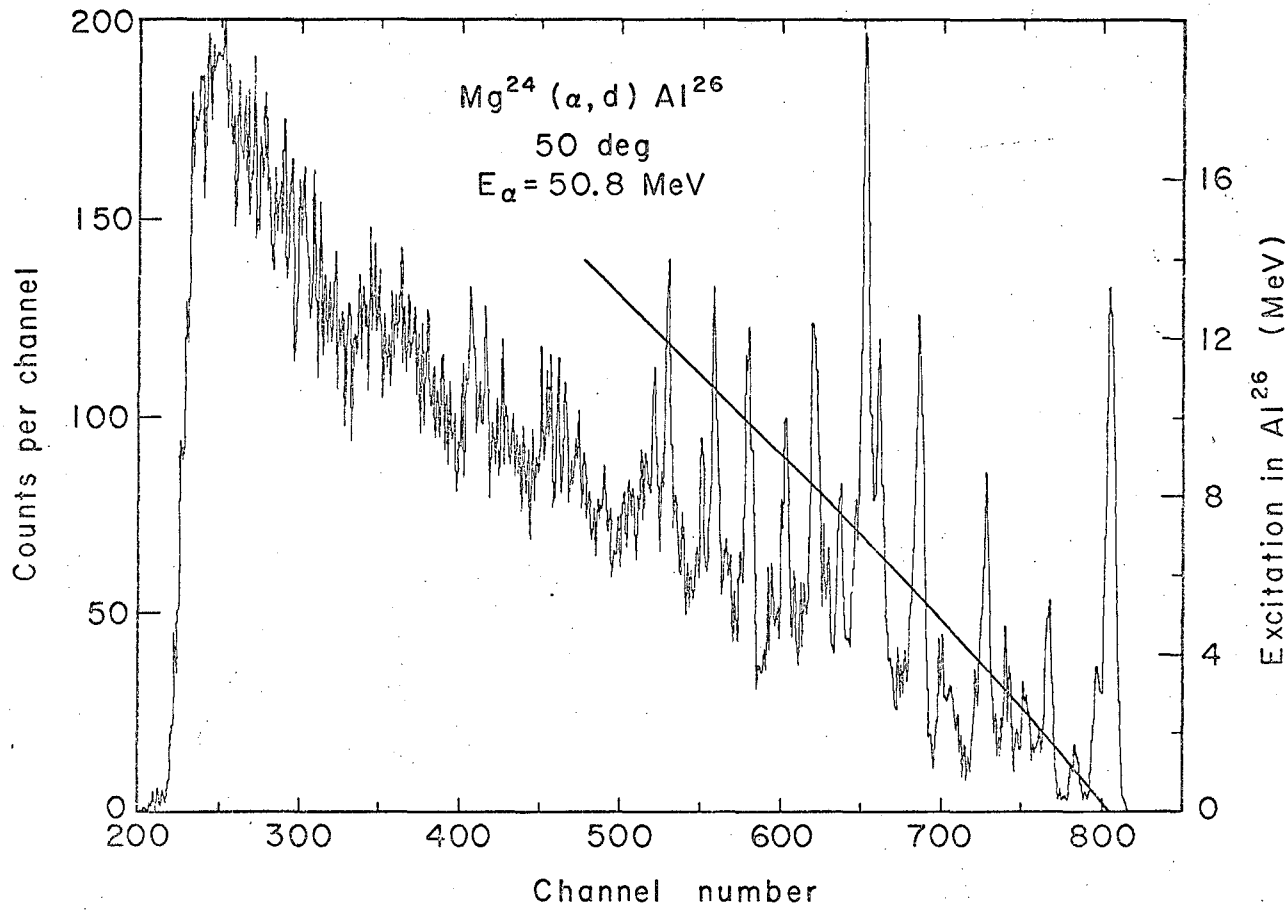

Fig. 11

MUB-6551

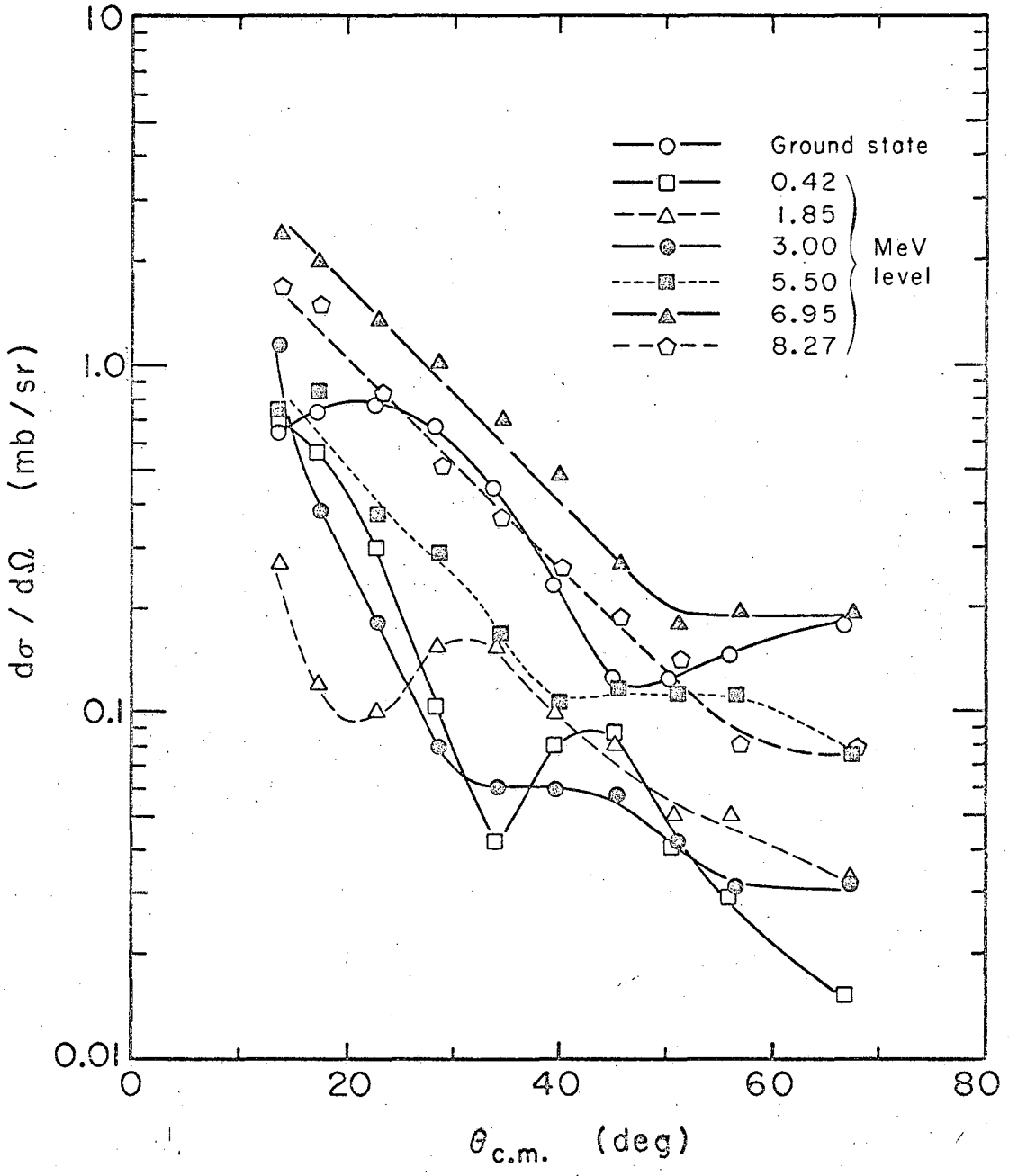

Fig. 12

MUB-6559

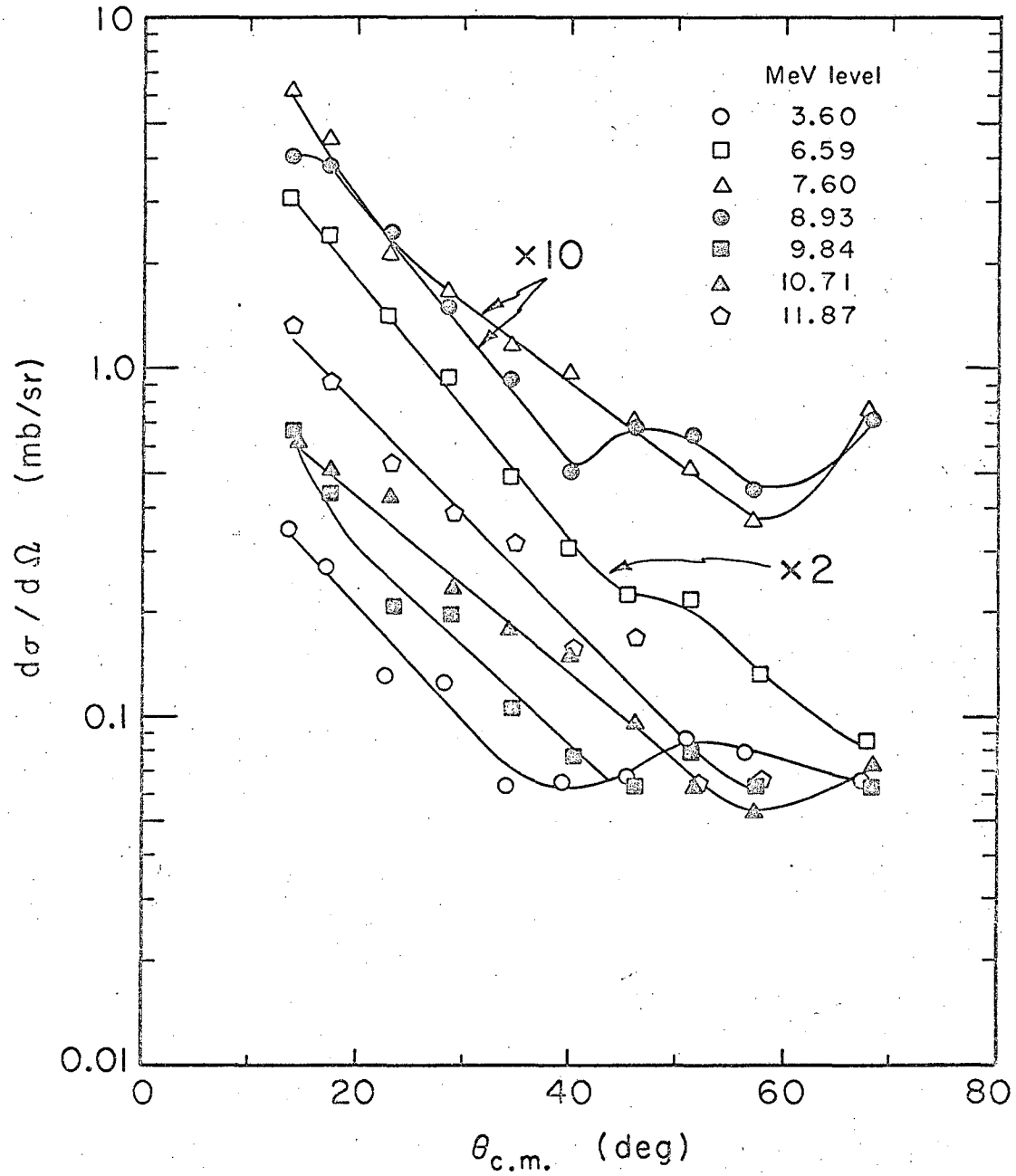

Fig. 13

MUB-6552

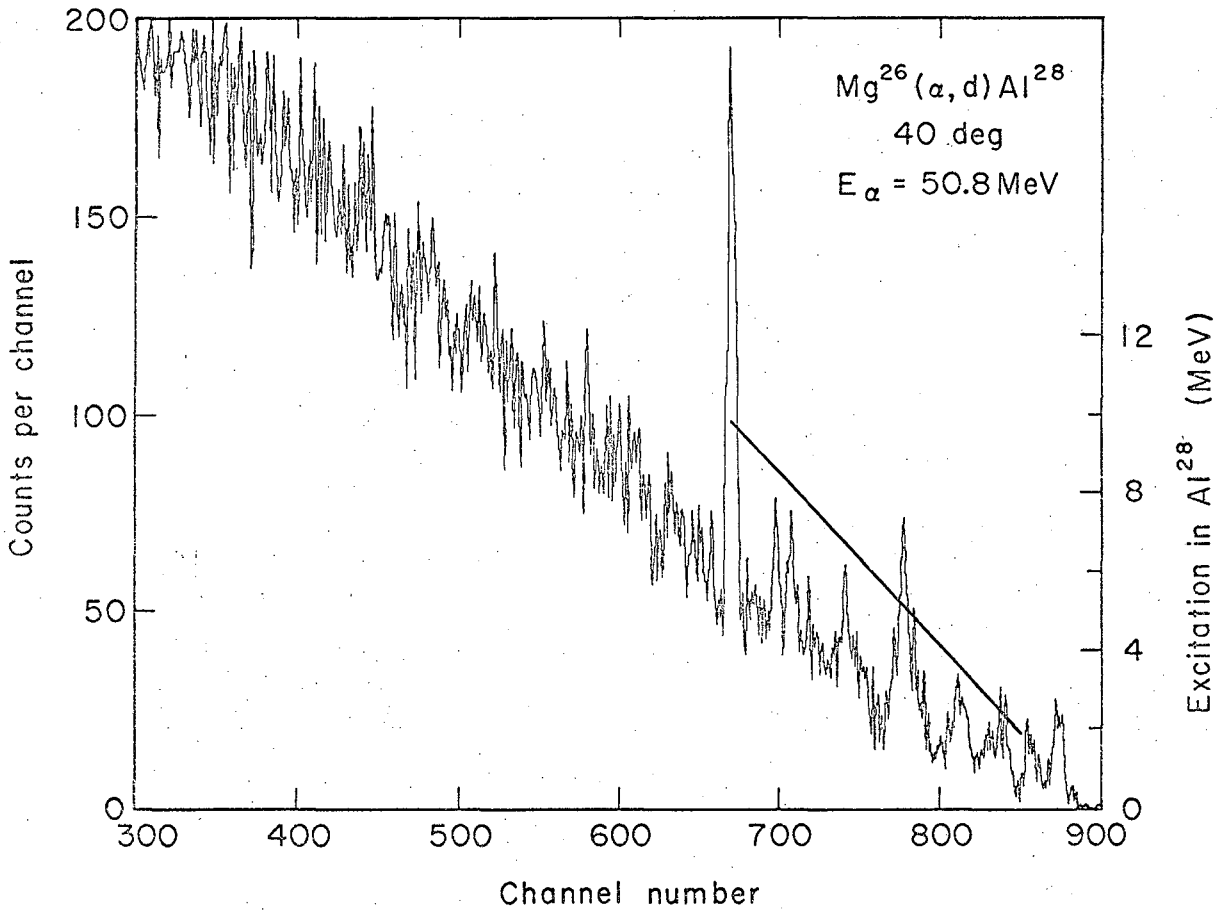

Fig. 14

MUB-6553

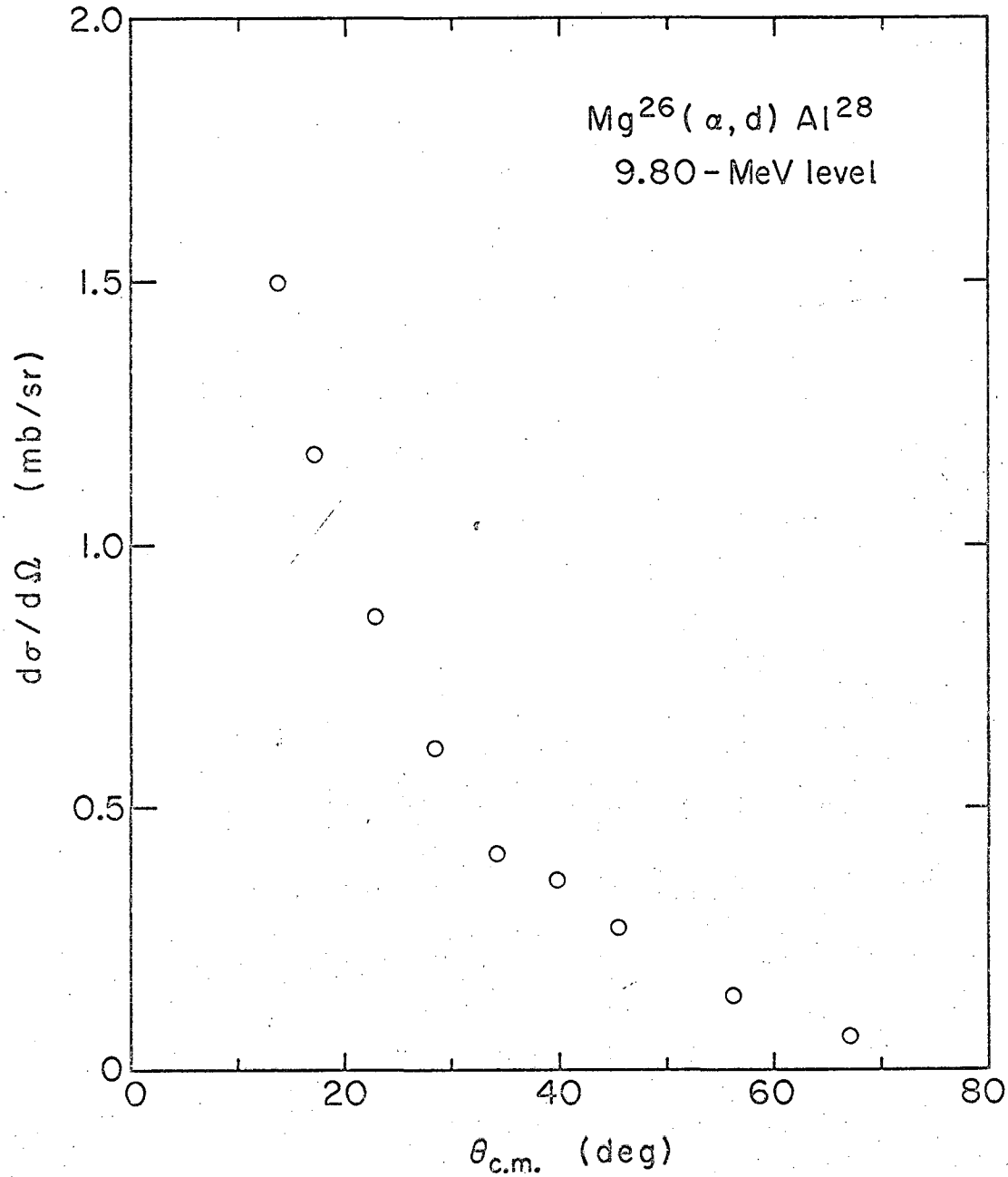

Fig. 15

MUB-6554

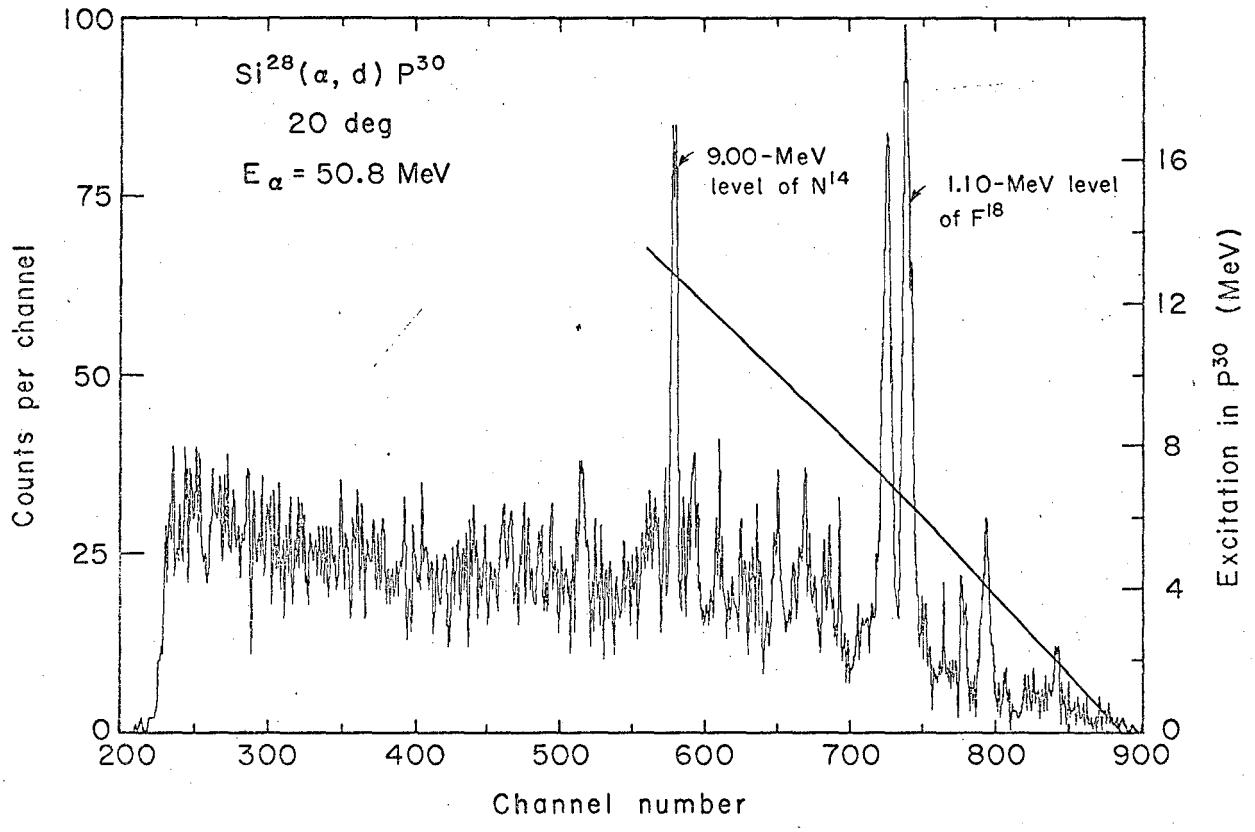

Fig. 16

MUB-6555

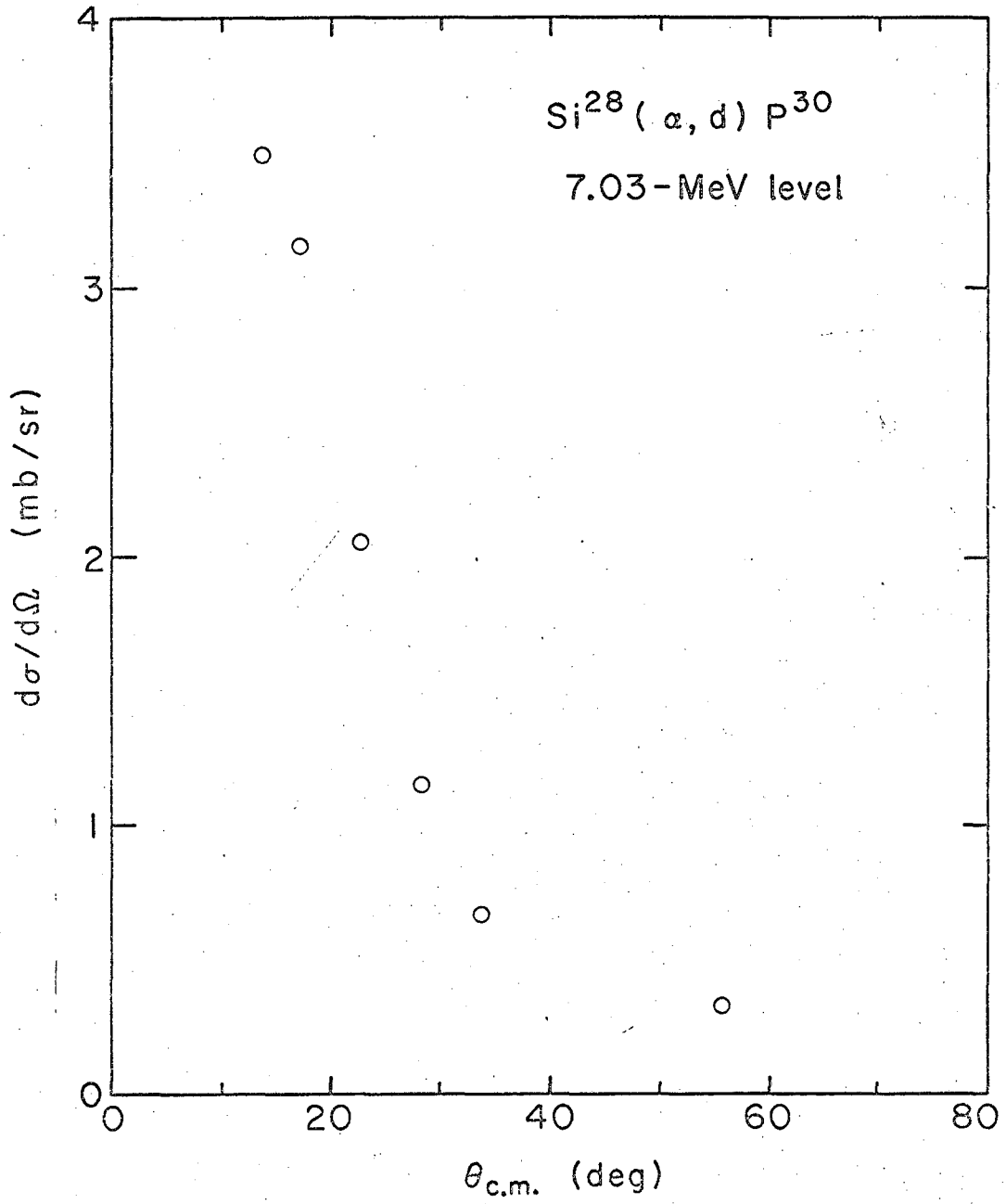

Fig. 17

MUB-6556

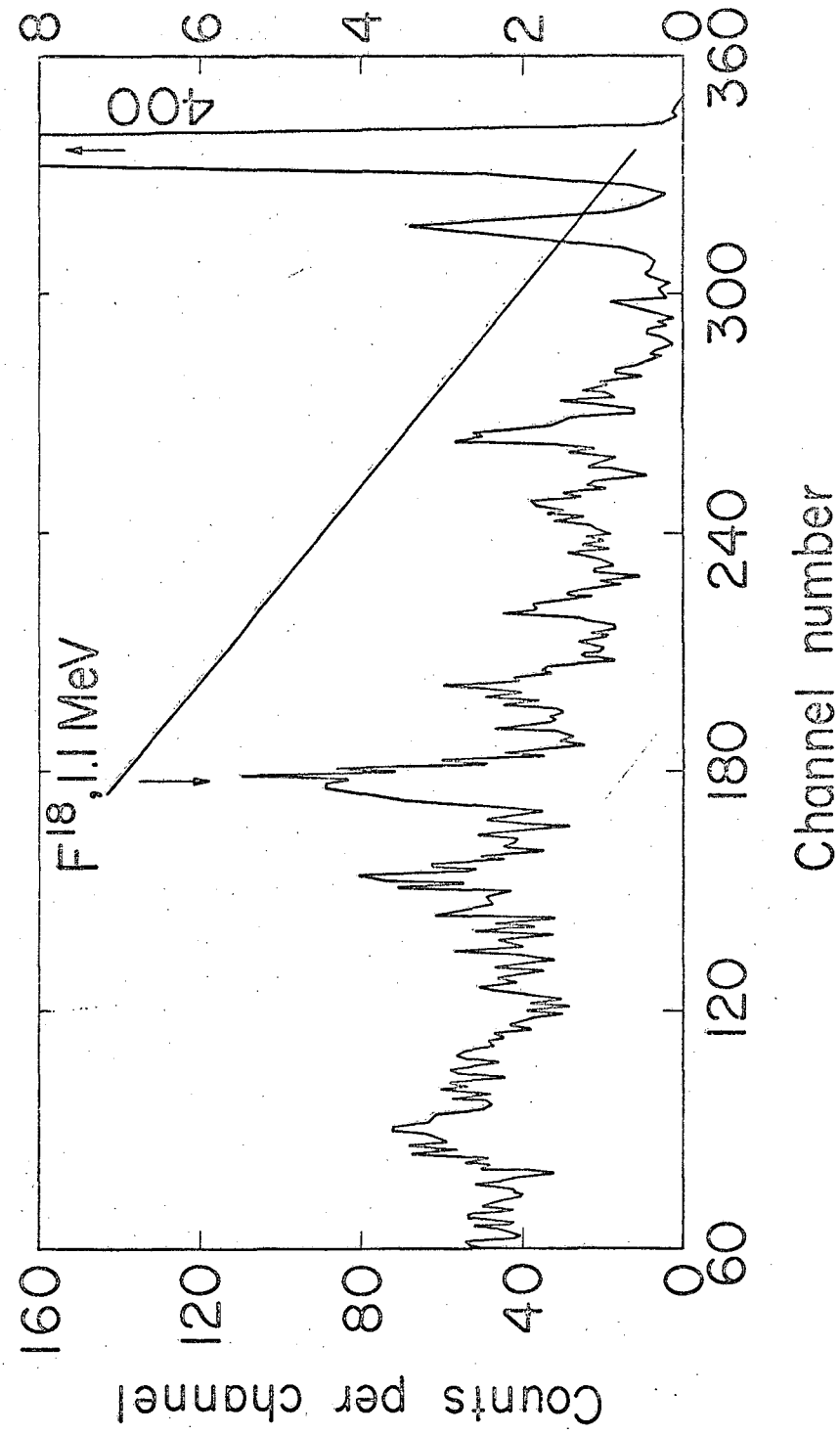

MUB-2373

Fig. 18

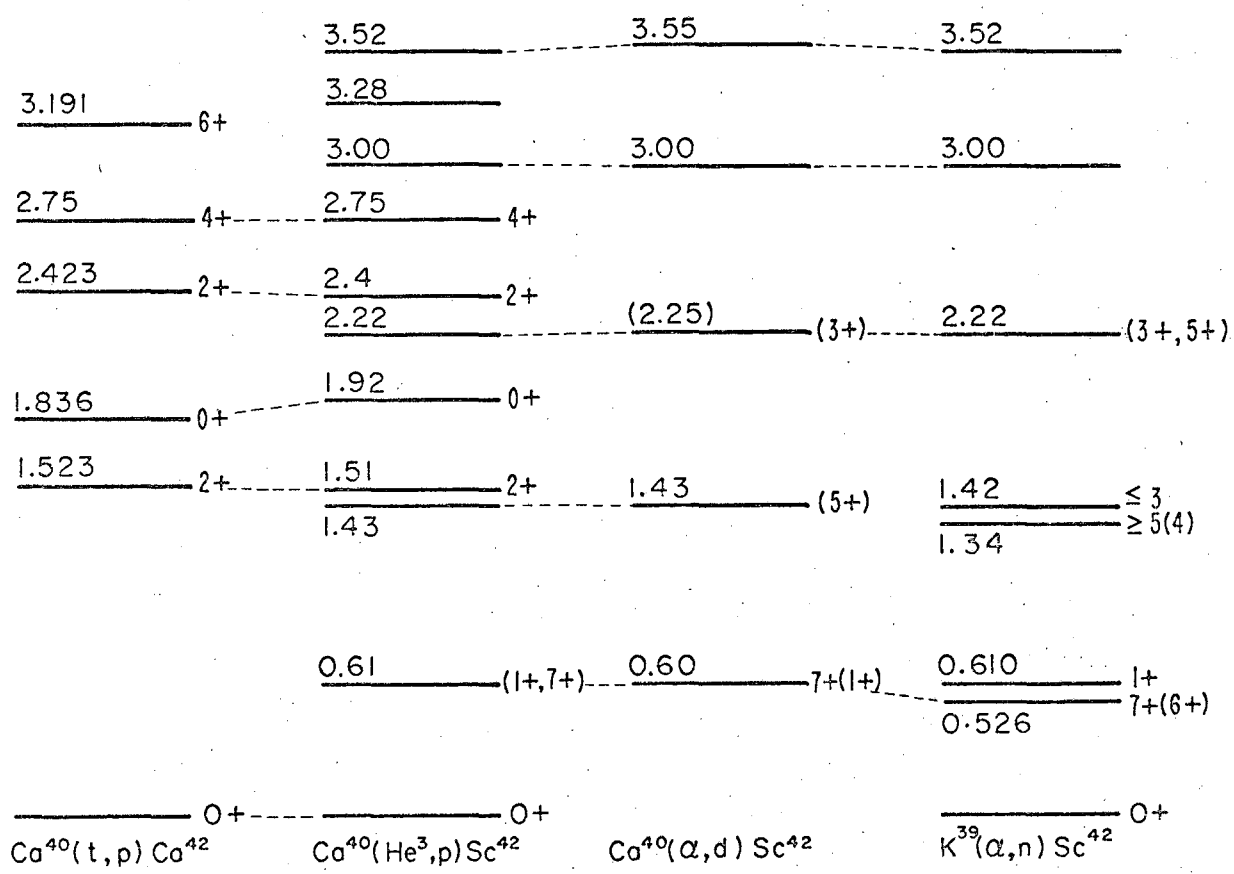

Fig. 19

MUB-6653

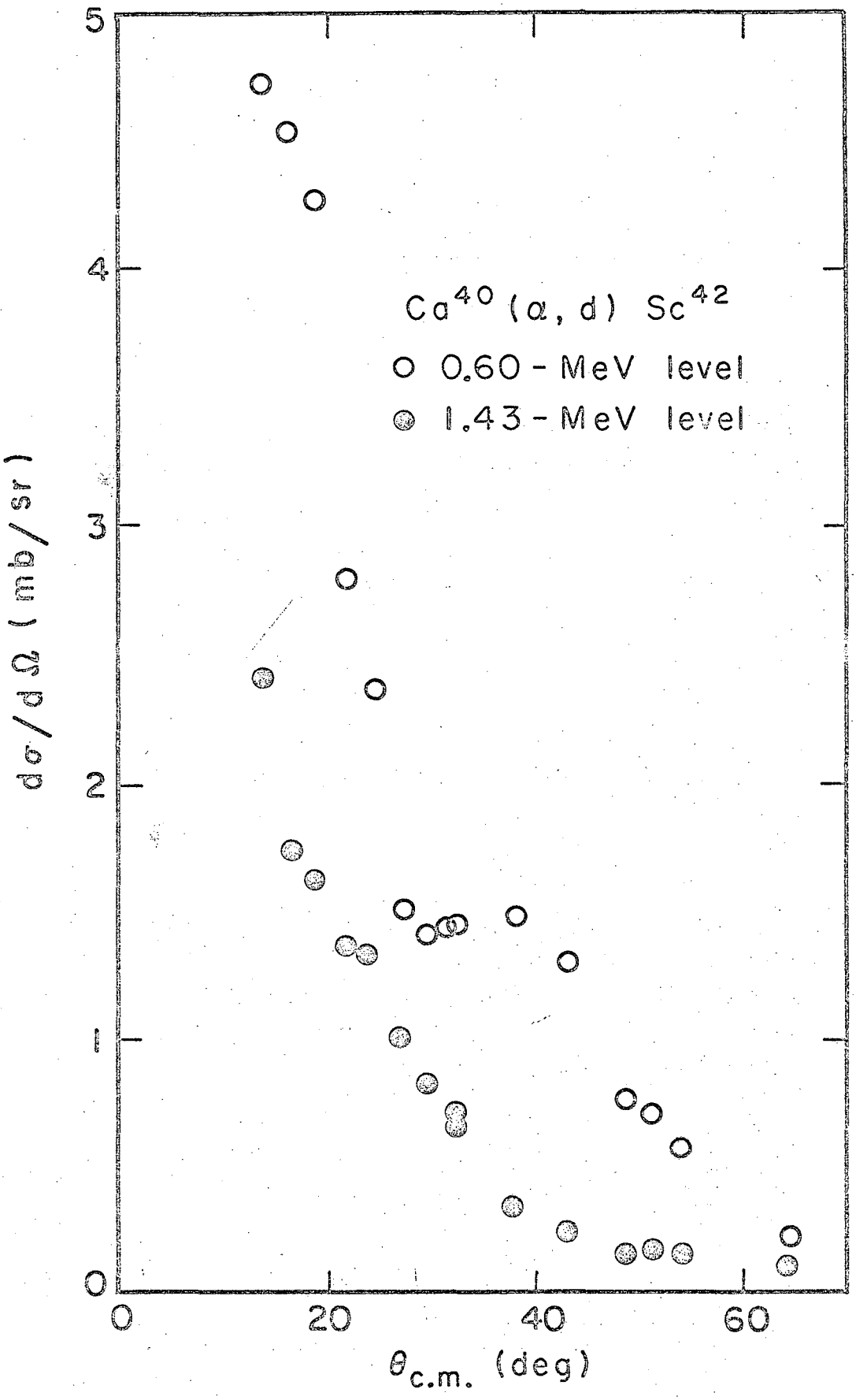

Fig. 20 MU-33936

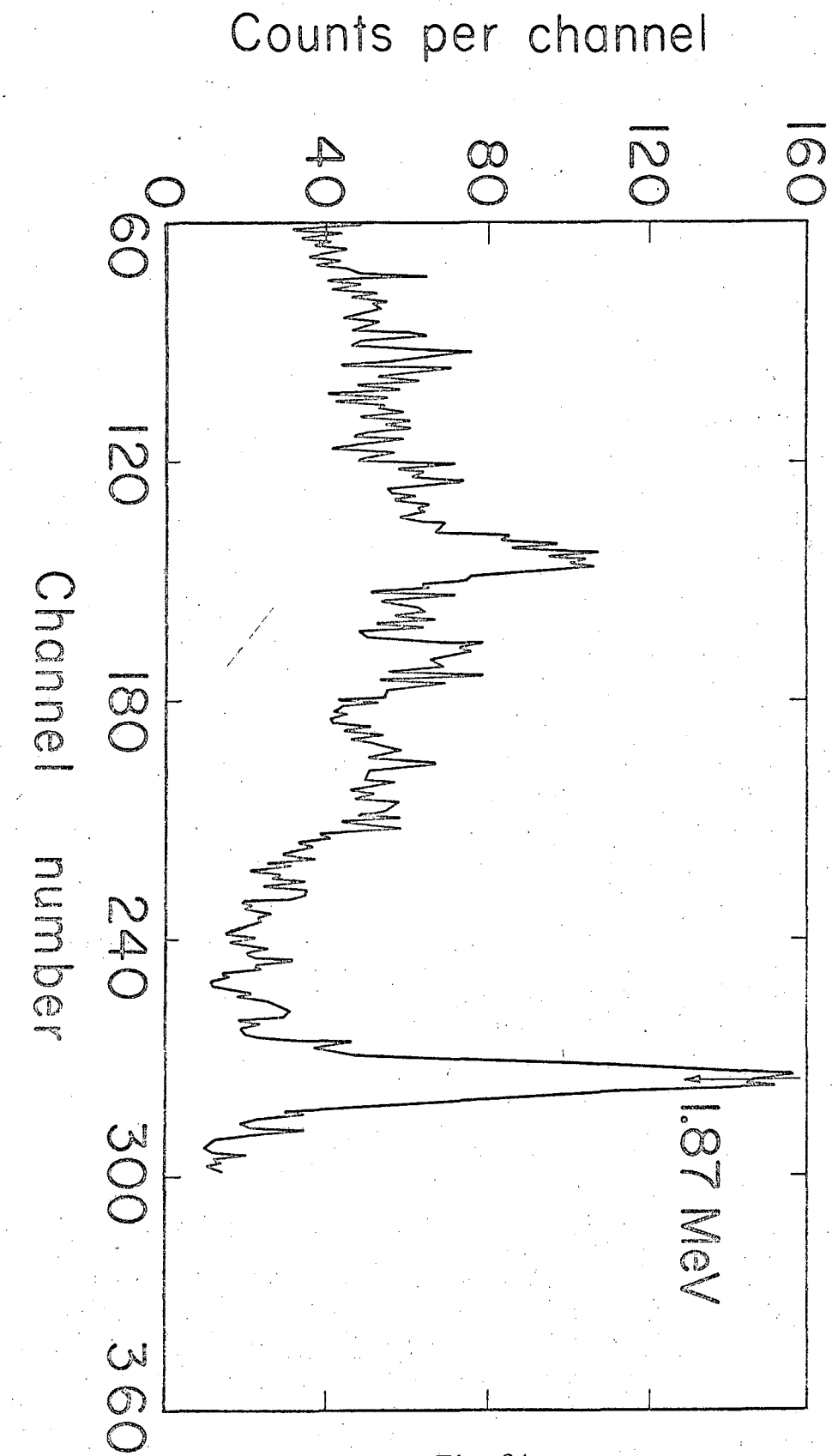

WU-33956

Fig. 21

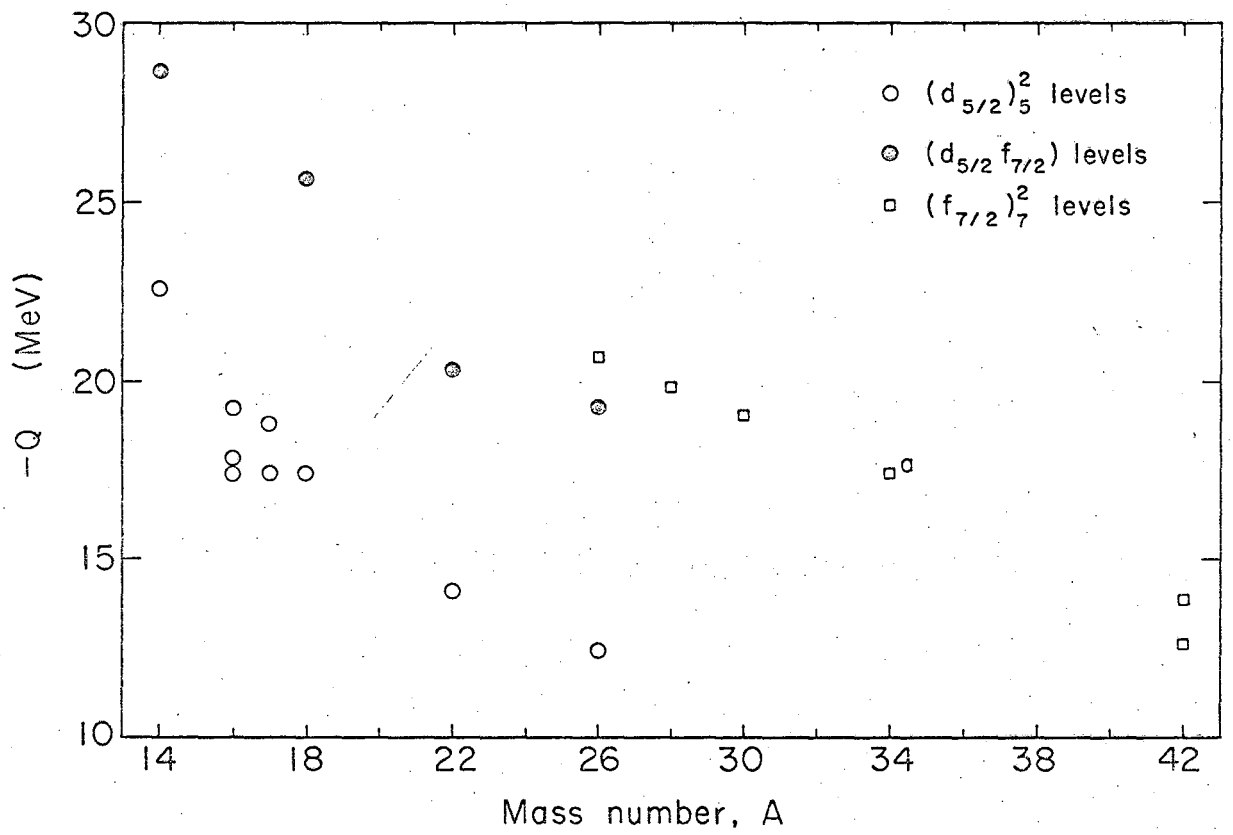

Fig. 22

MUB-6557

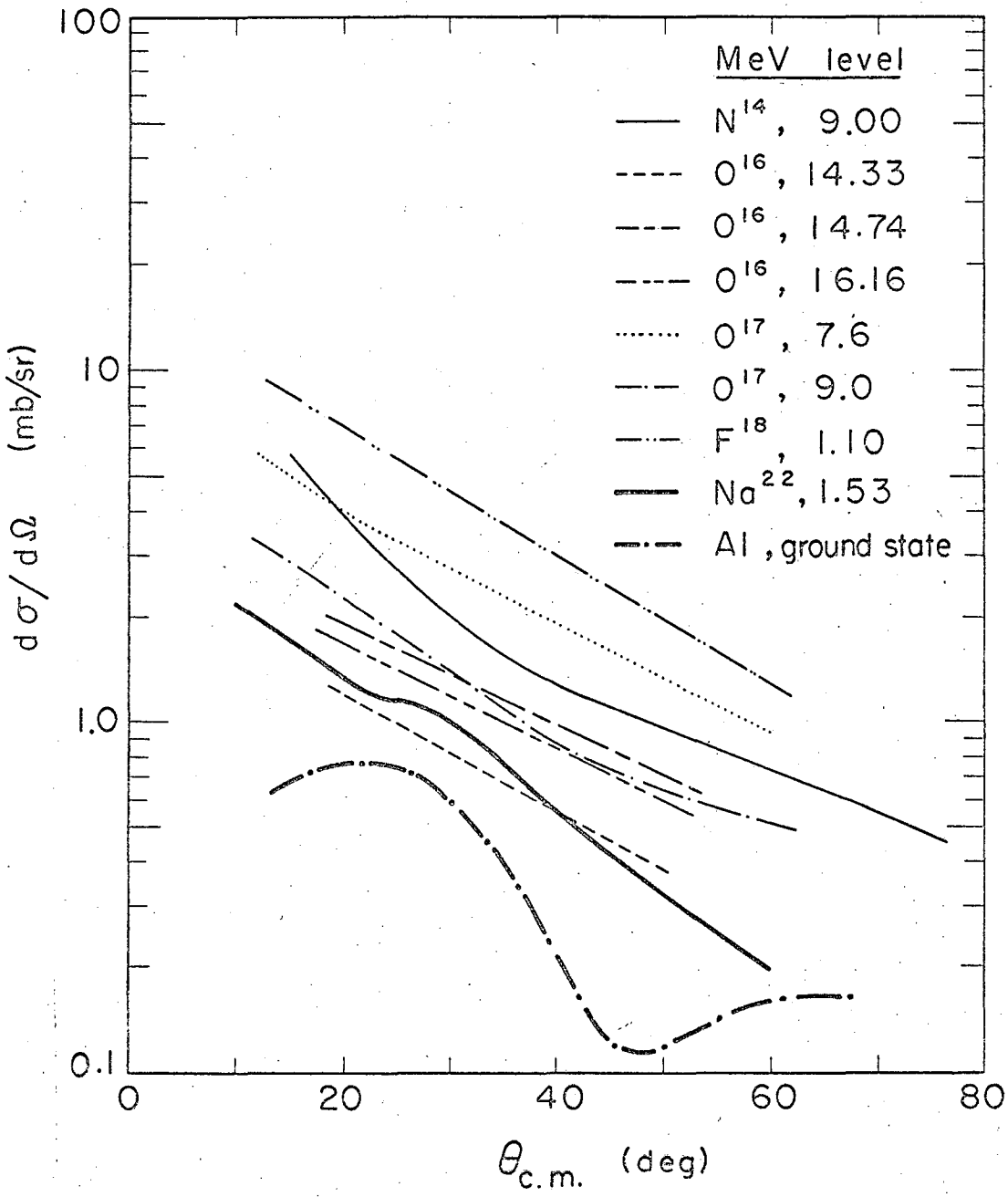

Fig. 23

MUB-6655

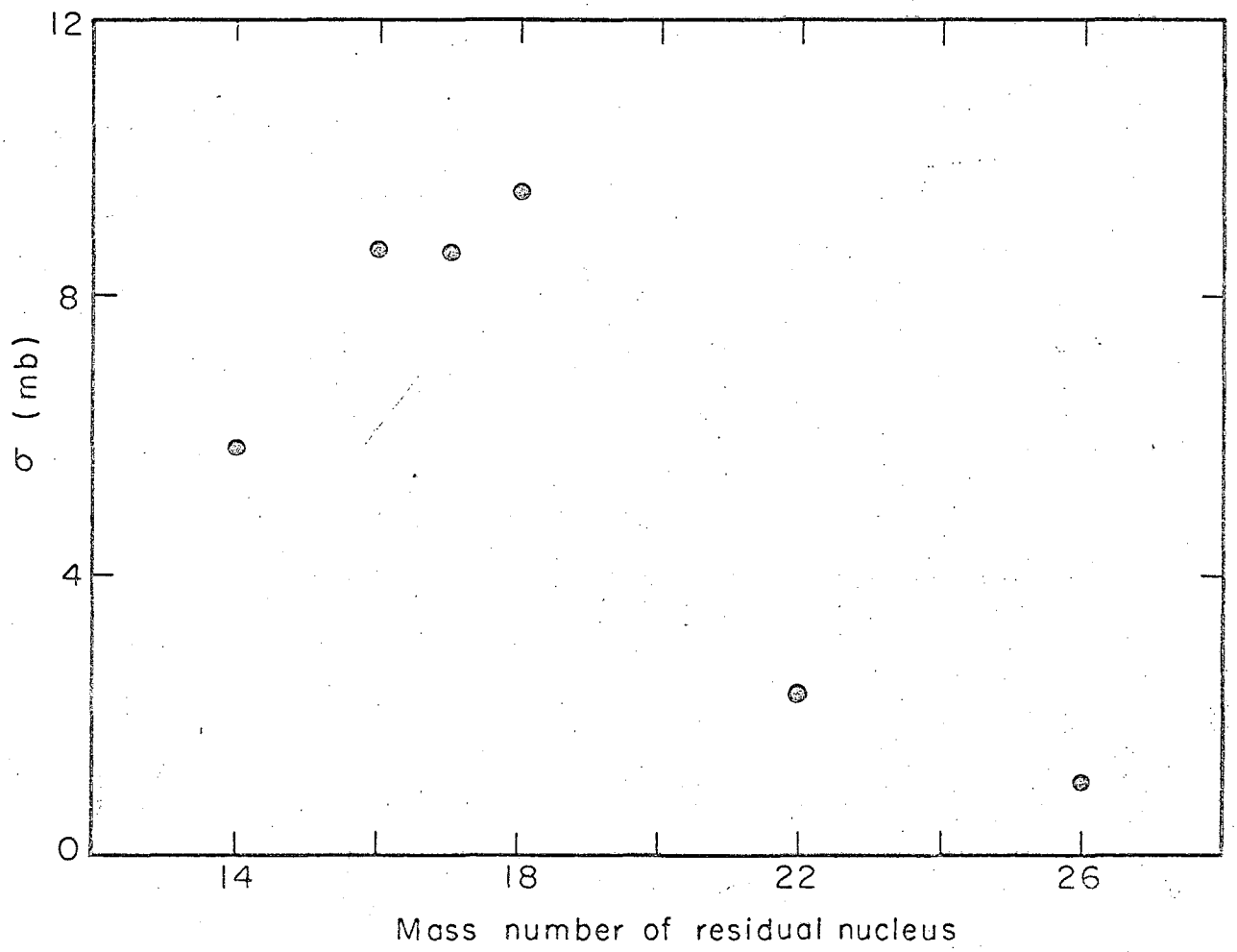

Fig. 24

MUB-6815

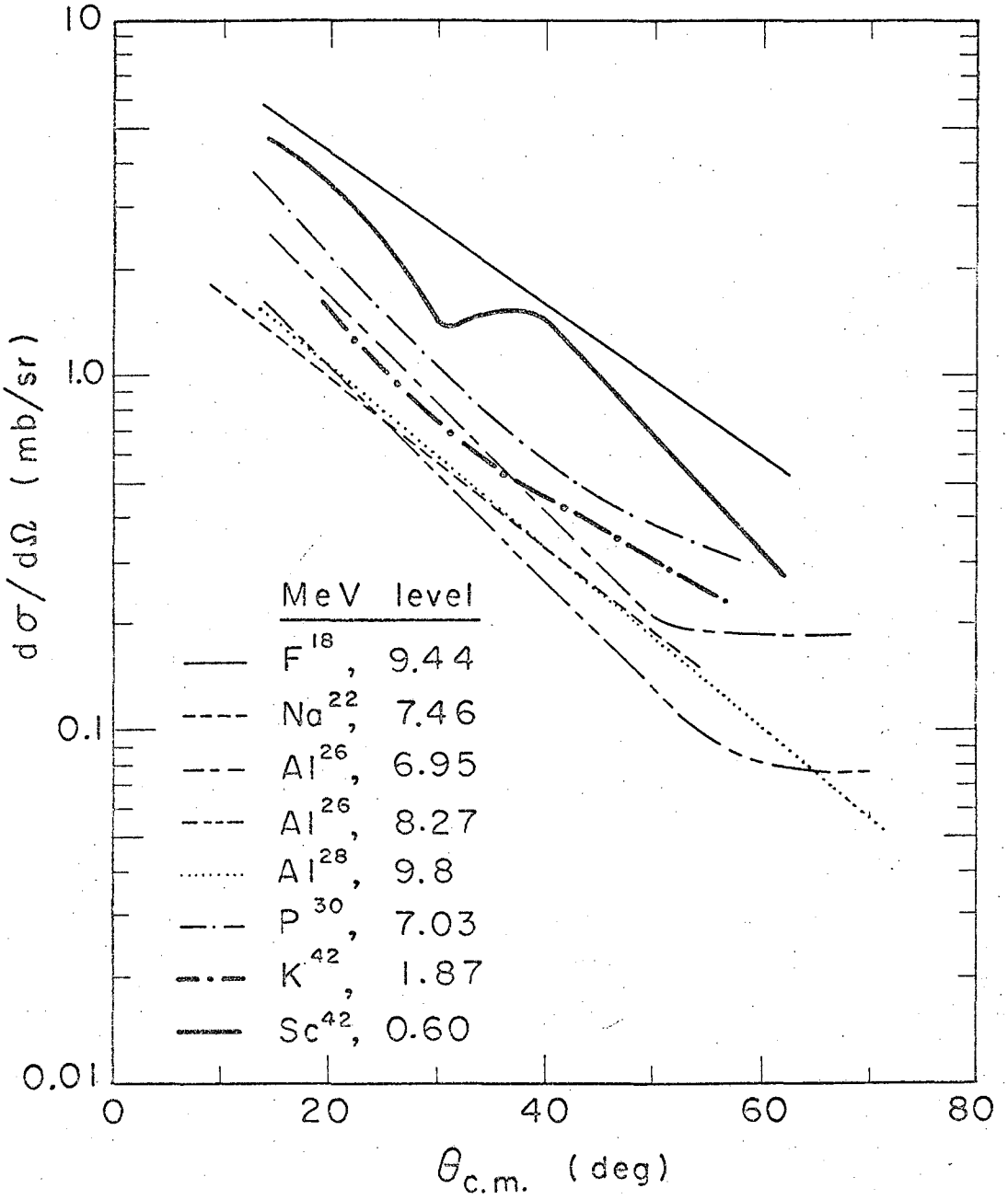

Fig. 25

MUB-6651

This report was prepared as an account of Government sponsored work. Neither the United States, nor the Commission, nor any person acting on behalf of the Commission:

A. Makes any warranty or representation, expressed or implied, with respect to the accuracy, completeness, or usefulness of the information contained in this report, or that the use of any information, apparatus, method, or process disclosed in this report may not infringe privately owned rights; or

B. Assumes any liabilities with respect to the use of, or for damages resulting from the use of any information, apparatus, method, or process disclosed in this report.

As used in the above, "person acting on behalf of the Commission" includes any employee or contractor of the Commission, or employee of such contractor, to the extent that such employee or contractor of the Commission, or employee of such contractor prepares, disseminates, or provides access to, any information pursuant to his employment or contract with the Commission, or his employment with such contractor.